Random matrix analysis of the QCD sign problem for general topology

JHEP03(2009)100

(http://iopscience.iop.org/1126-6708/2009/03/100)

JHEP

Published by IOP Publishing for SISSA

Received: *December 2, 2008*
Accepted: *January 16, 2009*
Published: *March 17, 2009*

Random matrix analysis of the QCD sign problem for general topology

Jacques Bloch and Tilo Wettig

Institute for Theoretical Physics, University of Regensburg, 93040 Regensburg, Germany

E-mail: jacques.bloch@physik.uni-regensburg.de, tilo.wettig@physik.uni-regensburg.de

Abstract: Motivated by the important role played by the phase of the fermion determinant in the investigation of the sign problem in lattice QCD at nonzero baryon density, we derive an analytical formula for the average phase factor of the fermion determinant for general topology in the microscopic limit of chiral random matrix theory at nonzero chemical potential, for both the quenched and the unquenched case. The formula is a nontrivial extension of the expression for zero topology derived earlier by Splittorff and Verbaarschot. Our analytical predictions are verified by detailed numerical random matrix simulations of the quenched theory.

Keywords: Matrix Models, Lattice QCD

ArXiv ePrint: 0812.0324

doi:10.1088/1126-6708/2009/03/100

JHEP03(2009)100

Contents

JHEP03(2009)100

1 Introduction

The theory of the strong interactions, also called Quantum Chromodynamics (QCD), describes the interactions between quarks and gluons and is responsible for the existence of hadrons. Lattice-regularized QCD allows for the description of low-energy properties and other nonperturbative phenomena in QCD and has the salient property that it can be systematically improved towards the continuum limit. In lattice QCD, space-time is discretized and the functional integral of the quantum field theory is performed by a Markov-chain Monte-Carlo method.

An important subject of study is the behavior of QCD in an environment exhibiting an abundance of particles over anti-particles. Such conditions arise, e.g., in astrophysical objects like neutron stars, and can be reproduced in heavy-ion collision experiments. Part of the interest comes from the existence of various phases in QCD, which are usually exemplified by means of the QCD phase diagram [1]. To study QCD at nonzero baryon density a quark chemical potential is introduced in the QCD Lagrangian. (In the following, we will omit the qualifier "quark" and only speak of a chemical potential.) In the presence of a chemical potential the QCD Dirac operator is no longer anti-Hermitian, i.e., its eigenvalues spread into the complex plane and its determinant will generically be complex.

In lattice QCD the effect of dynamical fermions can be integrated out, leaving behind the determinant of the Dirac operator. Dynamical lattice simulations for QCD at nonzero chemical potential are problematic because the fermion determinant is complex and hence its real part can be negative, which prohibits its incorporation in the weight of the Monte-Carlo sampling. This is the so-called sign problem, which also occurs in other theories and has been the subject of a large number of investigations in recent years (for an incomplete list see, e.g., refs. [2–9]). While many of these works are concerned with a solution of the sign problem by various clever ideas, here we concentrate on an analytical study of the sign problem, in the hope that the results we derive will contribute to its solution. The severeness of the sign problem depends on the magnitude of the chemical potential, and it is therefore illuminating to investigate the relation between the phase factor of the determinant and the chemical potential.

Chiral random matrix theory (chRMT) is a useful auxiliary in the study of the spectral properties of the Dirac operator in QCD [10–12]. Indeed, to leading order in the ε-regime of QCD the spectral properties of the Dirac operator are universal and can be described by chRMT [13]. In the presence of a chemical potential this correspondence is still valid even though the Dirac operator is now non-Hermitian. Appropriate random matrix models have been developed [14–17], and their correspondence with QCD at nonzero chemical potential was verified successfully, see ref. [18] for a review. The agreement of the microscopic spectral properties of the Dirac operator with the predictions of chiral random matrix theory has been confirmed for quenched lattice QCD simulations with chemical potential using the staggered operator [19], and more recently using the overlap operator [20, 21]. The latter operator has the interesting property that it satisfies the Ginsparg-Wilson relation and the trace anomaly at finite lattice spacing and can therefore have exact zero modes [22–27]. This allowed us to verify the predictions of chRMT at nonzero chemical potential for both

JHEP03(2009)100

zero and nonzero topology. The comparison between lattice QCD and chRMT also allows for a determination of the low-energy constants Σ and F of chiral perturbation theory.

Motivated by this agreement, we expect that a study of the behavior of the fermion determinant in chRMT will give us, in certain well-defined limits, important information about the sign problem that is encountered in dynamical QCD simulations at nonzero chemical potential. In ref. [28] Splittorff and Verbaarschot derived a solution for the average phase factor of the determinant in the microscopic limit of QCD (see section 3.2 for a description of this limit) for the case of trivial topology using chRMT at nonzero chemical potential. However, to compare the overlap data of ref. [20] with chRMT one also needs the RMT predictions for the average phase factor for general topology. The derivation of a formula for general topology is the main goal of this paper. As will be seen, the final expression contains two distinct parts. The first part is the generalization of the integrals representing the solution in ref. [28] from zero to arbitrary topology. The second part is a low-degree bivariate polynomial in mass and chemical potential which is absent for topological charge $\nu = 0$. For $\nu \neq 0$ it gives an important contribution to the average phase factor of the fermion determinant, especially for small mass. As the mass goes to zero only this term remains and completely determines the value of the average phase.

An important ingredient of the derivation is the ability to write the phase factor of the determinant as a ratio of characteristic polynomials. This quantity is recurrent in random matrix studies, both for theories with real [29, 30] and with complex eigenvalues [31], and its average can be computed in terms of Cauchy transforms of the orthogonal polynomials of the theory. To determine the phase factor of the determinant, the relevant Cauchy transform was computed in ref. [28] and expressed in terms of one-dimensional integrals for zero topology, i.e., for square random matrices. In the present paper we extend the solution of the Cauchy transform to the case of rectangular matrices. This solution could also be relevant for other applications, like those involving time series, where one matrix dimension is typically much larger than the other.

The structure of this paper is as follows. In section 2 we describe the chiral random matrix model at nonzero chemical potential. In section 3 we show how the microscopic limit of the phase of the fermion determinant, in both the quenched and the unquenched case, can be formally computed for such a matrix model in terms of a complex Cauchy transform integral. This two-dimensional integral is strongly oscillating, and in section 4 we apply and extend the method of ref. [28] to transform this integral into a much simpler and better behaved expression, involving only one-dimensional integrals and a short double sum (or bivariate polynomial). Explicit results for the quenched and unquenched cases as well as for the chiral and thermodynamic limits are given in section 5. In that section we also verify the analytical predictions for the quenched case by random matrix simulations for various values of the topological charge. We conclude in section 6. A number of technical details are worked out in several appendices.

JHEP03(2009)100

2 Non-Hermitian chiral random matrix model

To leading order in the ε-regime of QCD the spectral properties of the Dirac operator can be described by chRMT. In the presence of a chemical potential μ the Dirac operator D is no longer anti-Hermitian, and in the non-Hermitian chiral random matrix model introduced by Osborn [17] it takes the form

$$D(\mu) = \begin{pmatrix} 0 & i\Phi + \mu\Psi \\ i\Phi^\dagger + \mu\Psi^\dagger & 0 \end{pmatrix} , \tag{2.1}$$

where the matrices Φ and Ψ are complex random matrices of dimension $(N+\nu) \times N$, distributed according to the Gaussian weight function

$$w(X) = (N/\pi)^{N(N+\nu)} \exp\left(-N \operatorname{tr} X^\dagger X\right) . \tag{2.2}$$

For a detailed analysis of this model, see also ref. [32]. For the conversion of random matrix units to physical units, see the beginning of section 3.2.

The parameter N will be taken to infinity when computing the microscopic limit (see section 3.2). The matrix in eq. (2.1) has $|\nu|$ exact zero modes, which allows us to identify ν with the topological charge. In the following, we keep ν fixed as $N \to \infty$ and assume without loss of generality that $\nu \geq 0$. (For $\nu < 0$ we can simply replace ν by $|\nu|$ in the analytical results that will be computed below in the large-N limit.) The nonzero eigenvalues of $D(\mu)$ come in N pairs $(z_k, -z_k)$. For $\mu = 0$, the z_k are purely imaginary.

For fixed ν, the partition function of the random matrix model is given by

$$Z_\nu^{N_f}(\mu; \{m_f\}) = \int d\Phi d\Psi \, w(\Phi) w(\Psi) \prod_{f=1}^{N_f} \det\left(D(\mu) + m_f\right) , \tag{2.3}$$

where the integration measure is defined by

$$dX = \prod_{k=1}^{N+\nu} \prod_{\ell=1}^{N} d\operatorname{Re} X_{k\ell} d\operatorname{Im} X_{k\ell} , \tag{2.4}$$

N_f is the number of dynamical quarks, and the m_f are the quark masses. The quenched case corresponds to $N_f = 0$, i.e., the fermion determinants are absent.

To perform the integration over Φ and Ψ, it is convenient to go to an eigenvalue representation of the random matrix $D(\mu)$. As shown in ref. [17], the partition function can be rewritten, up to a normalization constant that depends on μ and ν, as an integral over the z_k,

$$Z_\nu^{N_f}(\alpha; \{m_f\}) = \int_{\mathbb{C}} \prod_{k=1}^{N} d^2 z_k \, w^\nu(z_k, z_k^*; \alpha) \, |\Delta_N(\{z^2\})|^2 \prod_{f=1}^{N_f} \left(m_f^2 - z_k^2\right) , \tag{2.5}$$

where we introduced $\alpha = \mu^2$, the integrals over the z_k are over the entire complex plane,

$$\Delta_N(\{z^2\}) \equiv \prod_{k>\ell} \left(z_k^2 - z_\ell^2\right) \tag{2.6}$$

is a Vandermonde determinant, the weight function is given by

$$w^\nu(z,z^*;\alpha) = |z|^{2\nu+2} \exp\left(-\frac{N(1-\alpha)}{4\alpha}(z^2+z^{*2})\right) K_\nu\left(\frac{N(1+\alpha)}{2\alpha}|z|^2\right) , \tag{2.7}$$

and K_ν is a modified Bessel function. The quenched partition function will be denoted by $Z_\nu(\alpha)$.

The ensemble average of an observable $\mathcal{O}$ is given by

$$\langle \mathcal{O} \rangle_{\nu,N_f} = \frac{1}{Z_\nu^{N_f}} \int_{\mathbb{C}} \prod_{k=1}^{N} d^2z_k \, w^\nu(z_k,z_k^*;\alpha) \, |\Delta_N\left(\{z^2\}\right)|^2 \prod_{f=1}^{N_f} \left(m_f^2 - z_k^2\right) \, \mathcal{O}(z_1,\ldots,z_N) \, . \tag{2.8}$$

When there is no danger of confusion we will omit one or both of the subscripts on $\langle \mathcal{O} \rangle$.

Our derivation will follow the general line of arguments given in ref. [28] for $\nu = 0$, with the necessary generalizations to arbitrary topology ν. To analyze the spectral properties of the random matrix model it is useful to introduce the orthogonal polynomials corresponding to the weight function (2.7) [17],

$$p_k^\nu(z;\alpha) = \left(\frac{1-\alpha}{N}\right)^k k! \, L_k^\nu\left(-\frac{Nz^2}{1-\alpha}\right) , \tag{2.9}$$

where $L_k^\nu(z)$ is the generalized or associated Laguerre polynomial of order ν and degree k. These orthogonal polynomials satisfy the orthogonality relation

$$\int_{\mathbb{C}} d^2z \, w^\nu(z,z^*;\alpha) p_k^\nu(z;\alpha) p_\ell^\nu(z;\alpha)^* = r_k^\nu(\alpha)\delta_{k\ell} \tag{2.10}$$

with norm

$$r_k^\nu(\alpha) = \frac{\pi\alpha(1+\alpha)^{2k+\nu} k!(k+\nu)!}{N^{2k+\nu+2}} \, . \tag{2.11}$$

For later use we also introduce the Cauchy transform of the orthogonal polynomials defined by

$$h_k^\nu(m;\alpha) = \int_{\mathbb{C}} \frac{d^2z}{z^2-m^2} w^\nu(z,z^*;\alpha) p_k^\nu(z;\alpha)^* \, . \tag{2.12}$$

3 Phase factor of the fermion determinant

3.1 The phase factor as a complex Cauchy transform

The Dirac operator describing a massive fermion is defined as $D(m;\mu) = D(\mu) + m\mathbb{1}$, where we assume that m is real. If we write its determinant as $\det D(m;\mu) = re^{i\theta}$, the phase factor can be extracted by forming the ratio

$$e^{2i\theta} = \frac{\det(D(\mu)+m)}{\det(D^\dagger(\mu)+m)} = \prod_{k=1}^{N} \frac{m^2-z_k^2}{m^2-z_k^{*2}} \, . \tag{3.1}$$

In this expression, m is the mass of a valence quark. From the physics point of view, an interesting quantity is the ensemble average of $e^{2i\theta}$ with two light dynamical quarks that have the same mass as the valence quark. This quantity tells us how the two-flavor determinant in the weight function oscillates. For simplicity, we shall refer to $e^{2i\theta}$ as the phase factor of the determinant, even though it is really the phase of the square of the determinant.

Because of the symmetries of (2.2), each matrix appears in the ensemble average with the same probability as its Hermitian conjugate. As the corresponding determinants are complex conjugate, the ensemble average of the phase factor is real. For strongly oscillating determinants the average phase factor will be close to zero, and the sign problem will be severe. On the other hand, for values of the chemical potential for which the average phase factor is close to unity one should still be able to perform dynamical simulations.

For each topic that is treated here and in the following sections, we will first address the quenched case and then generalize to the unquenched case. The virtue of this approach is that the quenched case already contains the essential ingredients, but the arguments and the notation can be kept simple. The generalization to the unquenched case is straightforward but leads to somewhat more complicated expressions.

3.1.1 Quenched case

The quenched ensemble average for the phase factor is given by

$$\begin{aligned}\left\langle e^{2i\theta}\right\rangle_{N_f=0} &= \left\langle \frac{\det(D(\mu)+m)}{\det(D^\dagger(\mu)+m)}\right\rangle_{N_f=0} = \frac{Z_\nu^{1|1^*}(\alpha,m)}{Z_\nu(\alpha)} \\ &= \frac{1}{Z_\nu(\alpha)}\int_{\mathbb{C}}\prod_{k=1}^{N} d^2z_k\, w^\nu(z_k,z_k^*;\alpha)\,|\Delta_N\left(\{z^2\}\right)|^2\frac{m^2-z_k^2}{m^2-z_k^{*2}}\,. \end{aligned} \tag{3.2}$$

The quantity $Z_\nu^{1|1^*}(\alpha,m)$ is the partition function of a random matrix model with one fermionic quark and one conjugate bosonic quark, see ref. [28] for a detailed discussion.

Using the formalism developed in refs. [31, 33], the quenched average of ratios of characteristic polynomials can be written in terms of the orthogonal polynomials (2.9) and their Cauchy transforms (2.12). Applying this formalism to the quenched average phase factor (3.2) gives the compact expression

$$\left\langle e^{2i\theta}\right\rangle_{N_f=0} = -\frac{1}{r^\nu_{N-1}(\alpha)}\begin{vmatrix} h^\nu_{N-1}(m;\alpha) & h^\nu_N(m;\alpha)\\ p^\nu_{N-1}(m;\alpha) & p^\nu_N(m;\alpha)\end{vmatrix}\,, \tag{3.3}$$

which is a complex integral over the orthogonal polynomials due to the Cauchy transforms. This expression (and its analog for the unquenched case, see section 3.1.2) will prove to be very useful to compute the phase factor. Inserting the Cauchy transform (2.12) in eq. (3.3) yields an integral over orthogonal polynomials,

$$\left\langle e^{2i\theta}\right\rangle_{N_f=0} = -\frac{1}{r^\nu_{N-1}(\alpha)}\int_{\mathbb{C}}\frac{d^2z}{z^2-m^2}w^\nu(z,z^*;\alpha)\begin{vmatrix} p^\nu_{N-1}(z^*;\alpha) & p^\nu_N(z^*;\alpha)\\ p^\nu_{N-1}(m;\alpha) & p^\nu_N(m;\alpha)\end{vmatrix}\,, \tag{3.4}$$

where we also used $p_k^\nu(z)^* = p_k^\nu(z^*)$. The well-known recurrence relation for the generalized Laguerre polynomials,

$$(k+1)L_{k+1}^\nu(x) = (k+1+\nu)L_k^\nu(x) - xL_k^{\nu+1}(x)\,, \tag{3.5}$$

translates into a recurrence relation for the p_k^ν defined in eq. (2.9),

$$p_{k+1}^\nu(z;\alpha) = (k+1+\nu)\left(\frac{1-\alpha}{N}\right)p_k^\nu(z;\alpha) + z^2 p_k^{\nu+1}(z;\alpha)\,. \tag{3.6}$$

Since the determinant remains unchanged when forming linear combinations of its columns, we can rewrite the phase factor (3.4) using the recurrence (3.6) as

$$\left\langle e^{2i\theta}\right\rangle_{N_f=0} = -\frac{1}{r_{N-1}^\nu(\alpha)}\int_{\mathbb{C}}\frac{d^2z}{z^2-m^2}w^\nu(z,z^*;\alpha)\begin{vmatrix} p_{N-1}^\nu(z^*;\alpha) & z^{*2}p_{N-1}^{\nu+1}(z^*;\alpha)\\ p_{N-1}^\nu(m;\alpha) & m^2 p_{N-1}^{\nu+1}(m;\alpha)\end{vmatrix}\,, \tag{3.7}$$

where all the orthogonal polynomials are now of equal degree.

3.1.2 Unquenched case

In the presence of N_f dynamical fermion flavors with masses $m_1,\ldots,m_{N_f}$, the phase factor for a valence quark of mass m is given by

$$\begin{aligned}\left\langle e^{2i\theta}\right\rangle_{N_f} &= \left\langle\frac{\det(D(\mu)+m)}{\det(D^\dagger(\mu)+m)}\right\rangle_{N_f}\\ &= \frac{1}{Z_\nu^{N_f}(\alpha;\{m_f\})}\int_{\mathbb{C}}\prod_{k=1}^{N}d^2z_k\,w^\nu(z_k,z_k^*;\alpha)\,|\Delta_N\left(\{z^2\}\right)|^2\frac{m^2-z_k^2}{m^2-z_k^{*2}}\prod_{f=1}^{N_f}\left(m_f^2-z_k^2\right)\,,\end{aligned} \tag{3.8}$$

where $Z_\nu^{N_f}(\alpha;\{m_f\})$ is given by eq. (2.5). This can be written as a ratio of two partition functions,

$$\left\langle e^{2i\theta}\right\rangle_{N_f} = \frac{Z_\nu^{N_f+1|1^*}(\alpha,m;\{m_f\})}{Z_\nu^{N_f}(\alpha;\{m_f\})}\,, \tag{3.9}$$

where, in analogy to eq. (3.2), $Z_\nu^{N_f+1|1^*}$ is the chRMT partition function with N_f+1 fermionic quarks and one conjugate bosonic quark. Both partition functions can be computed using the results of ref. [31], but to apply these results we need to change the normalization and divide both $Z_\nu^{N_f+1|1^*}$ and $Z_\nu^{N_f}$ by the quenched partition function. Then the partition functions can be interpreted as averages of ratios of characteristic polynomials in the quenched ensemble. Applying the formalism of ref. [31] to the numerator of eq. (3.9)

JHEP03(2009)100

(with modified normalization) we find

$$Z_\nu^{N_f+1|1^*}(\alpha,m;\{m_f\}) = -\frac{1}{r_{N-1}^\nu(\alpha)\Delta_{N_f+1}(m^2,\{m_f^2\})} \times \begin{vmatrix} h_{N-1}^\nu(m;\alpha) & h_N^\nu(m;\alpha) & \cdots & h_{N+N_f}^\nu(m;\alpha) \\ p_{N-1}^\nu(m;\alpha) & p_N^\nu(m;\alpha) & \cdots & p_{N+N_f}^\nu(m;\alpha) \\ p_{N-1}^\nu(m_1;\alpha) & p_N^\nu(m_1;\alpha) & \cdots & p_{N+N_f}^\nu(m_1;\alpha) \\ \vdots & \vdots & \vdots & \vdots \\ p_{N-1}^\nu(m_{N_f};\alpha) & p_N^\nu(m_{N_f};\alpha) & \cdots & p_{N+N_f}^\nu(m_{N_f};\alpha) \end{vmatrix}, \tag{3.10}$$

where the matrix in the determinant is of size $(N_f+2)\times(N_f+2)$. Substituting the definition of the Cauchy transform (2.12) gives

$$Z_\nu^{N_f+1|1^*}(\alpha,m;\{m_f\}) = -\frac{1}{r_{N-1}^\nu(\alpha)\Delta_{N_f+1}(m^2,\{m_f^2\})}\int\frac{d^2z}{z^2-m^2}w^\nu(z,z^*;\alpha) \times \begin{vmatrix} p_{N-1}^\nu(z^*;\alpha) & p_N^\nu(z^*;\alpha) & \cdots & p_{N+N_f}^\nu(z^*;\alpha) \\ p_{N-1}^\nu(m;\alpha) & p_N^\nu(m;\alpha) & \cdots & p_{N+N_f}^\nu(m;\alpha) \\ p_{N-1}^\nu(m_1;\alpha) & p_N^\nu(m_1;\alpha) & \cdots & p_{N+N_f}^\nu(m_1;\alpha) \\ \vdots & \vdots & \vdots & \vdots \\ p_{N-1}^\nu(m_{N_f};\alpha) & p_N^\nu(m_{N_f};\alpha) & \cdots & p_{N+N_f}^\nu(m_{N_f};\alpha) \end{vmatrix}. \tag{3.11}$$

With the recurrence relation (3.6) for the orthogonal polynomials this becomes

$$Z_\nu^{N_f+1|1^*}(\alpha,m;\{m_f\}) = -\frac{1}{r_{N-1}^\nu(\alpha)\Delta_{N_f+1}(m^2,\{m_f^2\})}\int\frac{d^2z}{z^2-m^2}w^\nu(z,z^*;\alpha) \times \begin{vmatrix} p_{N-1}^\nu(z^*;\alpha) & z^{*2}p_{N-1}^{\nu+1}(z^*;\alpha) & \cdots & (z^{*2})^{N_f+1}p_{N-1}^{\nu+N_f+1}(z^*;\alpha) \\ p_{N-1}^\nu(m;\alpha) & m^2p_{N-1}^{\nu+1}(m;\alpha) & \cdots & (m^2)^{N_f+1}p_{N-1}^{\nu+N_f+1}(m;\alpha) \\ p_{N-1}^\nu(m_1;\alpha) & m_1^2p_{N-1}^{\nu+1}(m_1;\alpha) & \cdots & (m_1^2)^{N_f+1}p_{N-1}^{\nu+N_f+1}(m_1;\alpha) \\ \vdots & \vdots & \vdots & \vdots \\ p_{N-1}^\nu(m_{N_f};\alpha) & m_{N_f}^2p_{N-1}^{\nu+1}(m_{N_f};\alpha) & \cdots & (m_{N_f}^2)^{N_f+1}p_{N-1}^{\nu+N_f+1}(m_{N_f};\alpha) \end{vmatrix}. \tag{3.12}$$

The denominator in eq. (3.9) (with modified normalization) can be written as [31]

$$Z_\nu^{N_f}(\alpha;\{m_f\}) = \frac{1}{\Delta_{N_f}(\{m_f^2\})}\begin{vmatrix} p_N^\nu(m_1;\alpha) & p_{N+1}^\nu(m_1;\alpha) & \cdots & p_{N+N_f-1}^\nu(m_1;\alpha) \\ p_N^\nu(m_2;\alpha) & p_{N+1}^\nu(m_2;\alpha) & \cdots & p_{N+N_f-1}^\nu(m_2;\alpha) \\ \vdots & \vdots & \vdots & \vdots \\ p_N^\nu(m_{N_f};\alpha) & p_{N+1}^\nu(m_{N_f};\alpha) & \cdots & p_{N+N_f-1}^\nu(m_{N_f};\alpha) \end{vmatrix}, \tag{3.13}$$

JHEP03(2009)100

and using the recurrence relation (3.6) for the orthogonal polynomials this can be rewritten as

$$Z_\nu^{N_f}(\alpha;\{m_f\}) = \frac{1}{\Delta_{N_f}(\{m_f^2\})} \times \begin{vmatrix} p_N^\nu(m_1;\alpha) & m_1^2 p_N^{\nu+1}(m_1;\alpha) & \cdots & (m_1^2)^{N_f-1} p_N^{\nu+N_f-1}(m_1;\alpha) \\ p_N^\nu(m_2;\alpha) & m_2^2 p_N^{\nu+1}(m_2;\alpha) & \cdots & (m_2^2)^{N_f-1} p_N^{\nu+N_f-1}(m_2;\alpha) \\ \vdots & \vdots & \vdots & \vdots \\ p_N^\nu(m_{N_f};\alpha) & m_{N_f}^2 p_N^{\nu+1}(m_{N_f};\alpha) & \cdots & (m_{N_f}^2)^{N_f-1} p_N^{\nu+N_f-1}(m_{N_f};\alpha) \end{vmatrix} . \tag{3.14}$$

3.2 Microscopic limit

Universal results, i.e., results that also apply to QCD, can be obtained from chRMT in the so-called microscopic regime. This regime is obtained by taking $N \to \infty$ while keeping the rescaled parameters $\hat{m} = 2Nm$, $\hat{m}_f = 2Nm_f$, and $\hat{\alpha} = 2N\alpha$ fixed, and rescaling the spectrum using $\hat{z} = 2Nz$. The rescaled random matrix parameters can be converted to the physical parameters z, m, and μ using the relations $\hat{z} = zV\Sigma$, $\hat{m} = mV\Sigma$, and $\hat{\alpha} = \hat{\mu}^2 = \mu^2 F^2 V$, where V is the four-volume.[1] Furthermore, the pion mass m_π can be introduced through the combination $\mu^2/m_\pi^2 = \hat{\mu}^2/2\hat{m}$, where we have used the Gell-Mann–Oakes–Renner relation $m_\pi^2 F^2 = 2m\Sigma$ (assuming equal quark masses).

We now introduce the microscopic limits (denoted by a subscript s) of the orthogonal polynomials, the norm, and the weight function, respectively. They are worked out in appendix A, and we obtain

$$p_s^\nu(\hat{z};\hat{\alpha}) \equiv \lim_{N\to\infty} \frac{e^N}{(2N)^{\nu+1/2}} p_{N-1}^\nu(\hat{z}/2N;\hat{\alpha}/2N) = \sqrt{\pi} e^{-\hat{\alpha}/2} \hat{z}^{-\nu} I_\nu(\hat{z}) , \tag{3.15}$$

$$r_s^\nu(\hat{\alpha}) \equiv \lim_{N\to\infty} (2N)^2 e^{2N} r_{N-1}^\nu(\hat{\alpha}/2N) = 4\pi^2 \hat{\alpha} e^{\hat{\alpha}} , \tag{3.16}$$

$$w_s^\nu(\hat{z},\hat{z}^*;\hat{\alpha}) \equiv \lim_{N\to\infty} (2N)^{2\nu+2} w^\nu(\hat{z}/2N,\hat{z}^*/2N;\hat{\alpha}/2N) = |\hat{z}|^{2(\nu+1)} e^{-\frac{\hat{z}^2+\hat{z}^{*2}}{8\hat{\alpha}}} K_\nu\left(\frac{|\hat{z}|^2}{4\hat{\alpha}}\right) . \tag{3.17}$$

3.2.1 Quenched case

In terms of the above definitions, the microscopic limit of the quenched average phase factor (3.7) is given by

$$\begin{aligned} \left\langle e_s^{2i\theta} \right\rangle_{N_f=0} &\equiv \lim_{N\to\infty} \left\langle e^{2i\theta} \right\rangle_{N_f=0,\hat{\alpha}/2N,\hat{m}/2N} \\ &= -\frac{1}{r_s^\nu(\hat{\alpha})} \int_{\mathbb{C}} \frac{d^2\hat{z}}{\hat{z}^2-\hat{m}^2} w_s^\nu(\hat{z},\hat{z}^*;\hat{\alpha}) \begin{vmatrix} p_s^\nu(\hat{z}^*;\hat{\alpha}) & \hat{z}^{*2} p_s^{\nu+1}(\hat{z}^*;\hat{\alpha}) \\ p_s^\nu(\hat{m};\hat{\alpha}) & \hat{m}^2 p_s^{\nu+1}(\hat{m};\hat{\alpha}) \end{vmatrix} . \end{aligned} \tag{3.18}$$

[1] To be more precise, one should distinguish random matrix parameters and physical parameters in the relations $2Nz_{\mathrm{RMT}} = \hat{z} = z_{\mathrm{phys}} V\Sigma$, $2Nm_{\mathrm{RMT}} = \hat{m} = m_{\mathrm{phys}} V\Sigma$, and $2N\mu_{\mathrm{RMT}}^2 = \hat{\mu}^2 = \mu_{\mathrm{phys}}^2 F^2 V$. This distinction makes it explicit that the limits $N \to \infty$ and $V \to \infty$ can be decoupled.

JHEP03(2009)100

As expected, the dependence on N has dropped out, leaving a finite microscopic limit for the average phase factor. Substituting the asymptotic results from eqs. (3.15)–(3.17) yields

$$\left\langle e_s^{2i\theta}\right\rangle_{N_f=0} = -\frac{e^{-2\hat{\alpha}}}{4\pi\hat{\alpha}\hat{m}^\nu}\int_{\mathbb{C}}\frac{d^2z}{z^2-\hat{m}^2}|z|^{2(\nu+1)}e^{-\frac{z^2+z^{*2}}{8\hat{\alpha}}} \times K_\nu\left(\frac{|z|^2}{4\hat{\alpha}}\right)(z^*)^{-\nu}\begin{vmatrix} I_\nu(z^*) & z^*I_{\nu+1}(z^*) \\ I_\nu(\hat{m}) & \hat{m}I_{\nu+1}(\hat{m})\end{vmatrix}, \tag{3.19}$$

where we renamed the integration variable $\hat{z}$ back to z. This equation can be rewritten compactly as

$$\left\langle e_s^{2i\theta}\right\rangle_{N_f=0} = \begin{vmatrix} \mathcal{H}_{\nu,0}(\hat{\alpha},\hat{m}) & \mathcal{H}_{\nu,1}(\hat{\alpha},\hat{m}) \\ I_\nu(\hat{m}) & \hat{m}I_{\nu+1}(\hat{m})\end{vmatrix}, \tag{3.20}$$

where we defined the integral

$$\mathcal{H}_{\nu,k}(\hat{\alpha},\hat{m}) \equiv -\frac{e^{-2\hat{\alpha}}}{4\pi\hat{\alpha}\hat{m}^\nu}\int_{\mathbb{C}}\frac{d^2z}{z^2-\hat{m}^2}|z|^{2(\nu+1)}e^{-\frac{z^2+z^{*2}}{8\hat{\alpha}}}K_\nu\left(\frac{|z|^2}{4\hat{\alpha}}\right)(z^*)^{-\nu+k}I_{\nu+k}(z^*)\,, \tag{3.21}$$

which is closely related to the microscopic limit of the Cauchy transform (2.12). For the quenched case, this integral is only needed for $k = 0, 1$, but as we shall see in the next subsection, in the unquenched case it will be needed for $k = 0, \ldots, N_f + 1$.

3.2.2 Unquenched case

We now take the microscopic limit of eqs. (3.12) and (3.14). In eq. (3.12), the Vandermonde determinant $\Delta_{N_f+1}(m^2, \{m_f^2\})$ is a product of $N_f(N_f+1)/2$ factors for which the microscopic limit yields a $(2N)^{N_f(N_f+1)}$ dependence on N, while the explicit mass and z^* factors in the determinant yield a factor $1/(2N)^{(N_f+1)(N_f+2)}$. After also introducing the microscopic limits (3.15), (3.16), and (3.17) for the orthogonal polynomials, their normalization factor, and the weight function, respectively, one finds

$$\begin{aligned} Z_{\nu,s}^{N_f+1|1^*}(\hat{\alpha},\hat{m};\{\hat{m}_f\}) = {} & -(2N)^{(2\nu+N_f)N_f/2}e^{-NN_f} \\ & \times \frac{\pi^{N_f/2}e^{-\hat{\alpha}(N_f/2+2)}}{4\pi\hat{\alpha}(\hat{m}\hat{m}_1\hat{m}_2\ldots\hat{m}_{N_f})^\nu\Delta_{N_f+1}(\hat{m}^2,\{\hat{m}_f^2\})} \\ & \times \int\frac{d^2z}{z^2-\hat{m}^2}|z|^{2(\nu+1)}(z^*)^{-\nu}K_\nu\left(\frac{|z|^2}{4\hat{\alpha}}\right)e^{-\frac{z^2+z^{*2}}{8\hat{\alpha}}} \\ & \times \begin{vmatrix} I_{\nu,0}(z^*) & I_{\nu,1}(z^*) & \cdots & I_{\nu,N_f+1}(z^*) \\ I_{\nu,0}(\hat{m}) & I_{\nu,1}(\hat{m}) & \cdots & I_{\nu,N_f+1}(\hat{m}) \\ I_{\nu,0}(\hat{m}_1) & I_{\nu,1}(\hat{m}_1) & \cdots & I_{\nu,N_f+1}(\hat{m}_1) \\ \vdots & \vdots & \vdots & \vdots \\ I_{\nu,0}(\hat{m}_{N_f}) & I_{\nu,1}(\hat{m}_{N_f}) & \cdots & I_{\nu,N_f+1}(\hat{m}_{N_f})\end{vmatrix}, \end{aligned} \tag{3.22}$$

where we have again renamed the integration variable from $\hat{z}$ back to z and introduced the notation

$$I_{\nu,k}(z) = z^k I_{\nu+k}(z)\,. \tag{3.23}$$

In the microscopic limit of eq. (3.14), the Vandermonde determinant yields a factor $(2N)^{(N_f-1)N_f}$ which exactly cancels the factor $1/(2N)^{(N_f-1)N_f}$ coming from the explicit mass factors in the determinant. After introducing the microscopic limit (3.15) of the orthogonal polynomials we find

$$Z^{N_f}_{\nu,s}(\hat{\alpha};\{\hat{m}_f\}) = (2N)^{(2\nu+N_f)N_f/2} e^{-NN_f} \frac{\pi^{N_f/2} e^{-\hat{\alpha}N_f/2}}{(\hat{m}_1\hat{m}_2\ldots\hat{m}_{N_f})^\nu \Delta_{N_f}(\{\hat{m}_f^2\})} \mathcal{D}^{N_f}_\nu(\{\hat{m}_f\}) \quad (3.24)$$

with

$$\mathcal{D}^{N_f}_\nu(\{\hat{m}_f\}) = \begin{vmatrix} I_{\nu,0}(\hat{m}_1) & I_{\nu,1}(\hat{m}_1) & \cdots & I_{\nu,N_f-1}(\hat{m}_1) \\ I_{\nu,0}(\hat{m}_2) & I_{\nu,1}(\hat{m}_2) & \cdots & I_{\nu,N_f-1}(\hat{m}_2) \\ \vdots & \vdots & \vdots & \vdots \\ I_{\nu,0}(\hat{m}_{N_f}) & I_{\nu,1}(\hat{m}_{N_f}) & \cdots & I_{\nu,N_f-1}(\hat{m}_{N_f}) \end{vmatrix} . \quad (3.25)$$

The microscopic limit of the average phase factor (3.9) is given by the ratio of eqs. (3.22) and (3.24). The dependence on N drops out to give

$$\begin{aligned} \left\langle e^{2i\theta}_s \right\rangle_{N_f} = & -\frac{e^{-2\hat{\alpha}}}{4\pi\hat{\alpha}\hat{m}^\nu \prod_{f=1}^{N_f}(\hat{m}_f^2-\hat{m}^2)\mathcal{D}^{N_f}_\nu(\{\hat{m}_f\})} \\ & \times \int \frac{d^2z}{z^2-\hat{m}^2}|z|^{2(\nu+1)}(z^*)^{-\nu} K_\nu\left(\frac{|z|^2}{4\hat{\alpha}}\right) e^{-\frac{z^2+z^{*2}}{8\hat{\alpha}}} \\ & \times \begin{vmatrix} I_{\nu,0}(z^*) & I_{\nu,1}(z^*) & \cdots & I_{\nu,N_f+1}(z^*) \\ I_{\nu,0}(\hat{m}) & I_{\nu,1}(\hat{m}) & \cdots & I_{\nu,N_f+1}(\hat{m}) \\ I_{\nu,0}(\hat{m}_1) & I_{\nu,1}(\hat{m}_1) & \cdots & I_{\nu,N_f+1}(\hat{m}_1) \\ \vdots & \vdots & \vdots & \vdots \\ I_{\nu,0}(\hat{m}_{N_f}) & I_{\nu,1}(\hat{m}_{N_f}) & \cdots & I_{\nu,N_f+1}(\hat{m}_{N_f}) \end{vmatrix} , \end{aligned} \quad (3.26)$$

which can be rewritten using the integral definition (3.21) as

$$\left\langle e^{2i\theta}_s \right\rangle_{N_f} = \frac{1}{\prod_{f=1}^{N_f}(\hat{m}_f^2-\hat{m}^2)\mathcal{D}^{N_f}_\nu(\{\hat{m}_f\})} \begin{vmatrix} \mathcal{H}_{\nu,0}(\hat{\alpha},\hat{m}) & \mathcal{H}_{\nu,1}(\hat{\alpha},\hat{m}) & \cdots & \mathcal{H}_{\nu,N_f+1}(\hat{\alpha},\hat{m}) \\ I_{\nu,0}(\hat{m}) & I_{\nu,1}(\hat{m}) & \cdots & I_{\nu,N_f+1}(\hat{m}) \\ I_{\nu,0}(\hat{m}_1) & I_{\nu,1}(\hat{m}_1) & \cdots & I_{\nu,N_f+1}(\hat{m}_1) \\ \vdots & \vdots & \vdots & \vdots \\ I_{\nu,0}(\hat{m}_{N_f}) & I_{\nu,1}(\hat{m}_{N_f}) & \cdots & I_{\nu,N_f+1}(\hat{m}_{N_f}) \end{vmatrix} . \quad (3.27)$$

We have thus reduced the problem of calculating the phase factor to the calculation of the two-dimensional integral $\mathcal{H}_{\nu,k}(\hat{\alpha},\hat{m})$ in eq. (3.21) for $k = 0,\ldots,N_f+1$. This integral will be computed in section 4.

3.2.3 Equal mass fermions

We now consider eq. (3.27) for the special case in which all dynamical fermions have the same mass $\hat{m}$ as the valence quark. To simplify the general expression we perform a Taylor

expansion of the entries $I_{\nu,k}(\hat{m}_f)$ of the determinant around $\hat{m}$,

$$I_{\nu,k}(\hat{m}_f) = I_{\nu,k}(\hat{m}) + \sum_{j=1}^{\infty} \frac{I^{(j)}_{\nu,k}(\hat{m})}{j!}(\hat{m}_f - \hat{m})^j \,, \qquad f = 1, \ldots, N_f \,. \tag{3.28}$$

Because a determinant remains unaltered when making linear combinations of its rows, we see that for each additional fermion it is sufficient to keep the next higher-order term in the expansion (3.28). The lower-order terms will not contribute as they are identical to the contribution from one of the previous fermions in the determinant, while the higher-order terms can be neglected as their contribution will vanish when $\hat{m}_f \to \hat{m}$. After taking each fermion mass in turn to $\hat{m}$, this leads to the simplified expression

$$\left\langle e_s^{2i\theta} \right\rangle_{N_f} = \frac{1}{(2\hat{m})^{N_f} N_f!} \frac{\begin{vmatrix} \mathcal{H}_{\nu,0}(\hat{\alpha},\hat{m}) & \mathcal{H}_{\nu,1}(\hat{\alpha},\hat{m}) & \cdots & \mathcal{H}_{\nu,N_f+1}(\hat{\alpha},\hat{m}) \\ I_{\nu,0}(\hat{m}) & I_{\nu,1}(\hat{m}) & \cdots & I_{\nu,N_f+1}(\hat{m}) \\ I'_{\nu,0}(\hat{m}) & I'_{\nu,1}(\hat{m}) & \cdots & I'_{\nu,N_f+1}(\hat{m}) \\ \vdots & \vdots & \vdots & \vdots \\ I^{(N_f)}_{\nu,0}(\hat{m}) & I^{(N_f)}_{\nu,1}(\hat{m}) & \cdots & I^{(N_f)}_{\nu,N_f+1}(\hat{m}) \end{vmatrix}}{\begin{vmatrix} I_{\nu,0}(\hat{m}) & I_{\nu,1}(\hat{m}) & \cdots & I_{\nu,N_f-1}(\hat{m}) \\ I'_{\nu,0}(\hat{m}) & I'_{\nu,1}(\hat{m}) & \cdots & I'_{\nu,N_f-1}(\hat{m}) \\ \vdots & \vdots & \vdots & \vdots \\ I^{(N_f-1)}_{\nu,0}(\hat{m}) & I^{(N_f-1)}_{\nu,1}(\hat{m}) & \cdots & I^{(N_f-1)}_{\nu,N_f-1}(\hat{m}) \end{vmatrix}} \,. \tag{3.29}$$

An alternative way to write this result is

$$\left\langle e_s^{2i\theta} \right\rangle_{N_f} = \frac{1}{(2\hat{m})^{N_f} N_f!} \frac{\mathcal{W}_{N_f}(\hat{\alpha},\hat{m})}{W_{N_f}(0,1,\ldots,N_f-1)} \,, \tag{3.30}$$

where we have defined

$$\mathcal{W}_{N_f}(\hat{\alpha},\hat{m}) = \sum_{k=0}^{N_f+1} (-)^k \mathcal{H}_{\nu,k}(\hat{\alpha},\hat{m}) W_{N_f+1}(0,\ldots,k-1,k+1,\ldots,N_f+1) \tag{3.31}$$

as a sum of Wronskians of order $N_f + 1$ with indices ranging from 0 to $N_f + 1$, where in each term a different index k is absent. The Wronskian

$$W_n(I_{\nu,k_1}(\hat{m}),\ldots,I_{\nu,k_n}(\hat{m})) = \begin{vmatrix} I_{\nu,k_1}(\hat{m}) & I_{\nu,k_2}(\hat{m}) & \cdots & I_{\nu,k_n}(\hat{m}) \\ I'_{\nu,k_1}(\hat{m}) & I'_{\nu,k_2}(\hat{m}) & \cdots & I'_{\nu,k_n}(\hat{m}) \\ \vdots & \vdots & \vdots & \vdots \\ I^{(n-1)}_{\nu,k_1}(\hat{m}) & I^{(n-1)}_{\nu,k_2}(\hat{m}) & \cdots & I^{(n-1)}_{\nu,k_n}(\hat{m}) \end{vmatrix} \tag{3.32}$$

that appears in eqs. (3.30) and (3.31) has been abbreviated by $W_n(k_1,\ldots,k_n)$.

JHEP03(2009)100

4 Evaluation of the complex Cauchy transform

4.1 Asymptotic behavior

To investigate the two-dimensional integral (3.21) it is instructive to first study the asymptotic behavior of the integrand. For large values of its argument the K-Bessel function behaves like [34, eq. (9.7.2)]

$$K_\nu(z) \sim \sqrt{\frac{\pi}{2z}} e^{-z} \,. \tag{4.1}$$

Here and in the rest of the paper we use the $\sim$ symbol for the leading-order term in an expansion for small or large argument, including all prefactors. To find the asymptotic behavior of the I-Bessel function we first note that the modified Bessel functions satisfy the relation [35, eq. (7.11.45)]

$$K_\nu(ze^{\pm i\pi}) = (-)^\nu K_\nu(z) \mp i\pi I_\nu(z) \,. \tag{4.2}$$

As the K-Bessel function has a branch cut along the negative real axis, it is convenient to adopt the convention $\arg(z) \in (-\pi, \pi]$ for the complex variable z. According to this convention, reversing the sign of $z = re^{i\theta}$ yields

$$-z = \begin{cases} re^{i(\theta-\pi)} & \text{for } \theta \in (0, \pi] \,, \\ re^{i(\theta+\pi)} & \text{for } \theta \in (-\pi, 0] \,, \end{cases} \tag{4.3}$$

such that $-z$ also has its argument in $(-\pi, \pi]$. Combining eqs. (4.2) and (4.3) gives the relation

$$I_\nu(z) = \frac{i\eta(z)}{\pi}\big((-)^\nu K_\nu(z) - K_\nu(-z)\big) \tag{4.4}$$

with

$$\eta(z) = \begin{cases} +1 & \text{for } \arg(z) \in (0, \pi] \,, \\ -1 & \text{for } \arg(z) \in (-\pi, 0] \,. \end{cases} \tag{4.5}$$

Alternative definitions for $\eta(z)$ are $i\eta(z) = \sqrt{z}/\sqrt{-z}$ or $\eta(z) = \operatorname{sgn}(\operatorname{Im} z)$, the latter only for $z \notin \mathbb{R}$. Substituting eq. (4.1) in eq. (4.4) gives the asymptotic formula[2]

$$I_\nu(z) \sim \frac{i\eta(z)}{\sqrt{2\pi}}\left((-)^\nu \frac{e^{-z}}{\sqrt{z}} - \frac{e^z}{\sqrt{-z}}\right) = \frac{1}{\sqrt{2\pi}}\left((-)^\nu \frac{e^{-z}}{\sqrt{-z}} + \frac{e^z}{\sqrt{z}}\right) , \tag{4.6}$$

where we used $i\eta(z) = \sqrt{z}/\sqrt{-z}$ to derive the last expression. With eqs. (4.1) and (4.6), the asymptotic behavior of the integrand in eq. (3.21) is proportional to

$$\frac{|z|^{2\nu+1}}{z^2 - \hat{m}^2} e^{-\frac{x^2}{2\hat{\alpha}}} (z^*)^{-\nu+k}\left((-)^{\nu+k}\frac{e^{-z^*}}{\sqrt{-z^*}} + \frac{e^{z^*}}{\sqrt{z^*}}\right) , \tag{4.7}$$

[2]Note that the asymptotic formula (9.7.1) in ref. [34] only contains the second term of eq. (4.6) and cannot be used here as it is only valid for $|\arg z| < \pi/2$.

where $z = x + iy$. Along the x-direction the integrand of the two-dimensional integral decreases like a Gaussian with width $\sqrt{\hat{\alpha}}$. However, in the y-direction the integrand oscillates very rapidly inside an envelope that goes like $y^{\nu+k-3/2}$. Eqs. (3.20) and (3.27) contain terms with $\nu + k \geq 1$, for which the integral (3.21) will diverge unless some particular cancellations occur due to the oscillatory behavior of the integrand. As the integral represents an observable quantity in random matrix theory we do expect such cancellations to obtain a finite result.

An instructive numerical exercise is the direct computation of the two-dimensional integral over the generalized Laguerre polynomials for finite N, as given in eq. (3.7) for the quenched case. Although Mathematica can only handle the numerical integration for $N \lesssim 30$ because of the strong oscillations, the results for $N = 1, \ldots, 30$ show a clear convergence towards a finite microscopic limit. (These numerical results also agree with the simulations presented in section 5.5.) This clearly indicates that eq. (3.19) is perfectly sane, even though the evaluation of the integral is nontrivial.

4.2 Change of integration path and transformation of variables

The main problem is to find a way to integrate over the oscillatory behavior in the y-direction. For $\nu = 0$ a method was devised in ref. [28] in which the integration along the real y-axis in the original (x, y)-plane was deformed to an integration path in the complex y-plane. This results in a well-behaved one-dimensional integral. Here, we show how this derivation can be generalized to $\nu \neq 0$, where proper care has to be taken of an additional singularity occurring in the integration domain.

The two terms e^{-z^*} and e^{z^*} in eq. (4.7) behave differently for $|y| \to \infty$. The first term decreases exponentially in the upper half of the complex y-plane and diverges exponentially in the lower half, whereas the second term behaves the other way around. Rather than treating these two terms separately, we can use eq. (4.4) to simplify eq. (3.21). Because of the $z \to -z$ symmetry of the integrand in (3.21), the two terms in (4.4) give the same contribution to the integral, and we obtain

$$\begin{aligned}\mathcal{H}_{\nu,k}(\hat{\alpha}, \hat{m}) = -\frac{ie^{-2\hat{\alpha}}}{2\pi^2 \hat{\alpha} \hat{m}^\nu} \int_{\mathbb{C}} \frac{d^2z}{z^2 - \hat{m}^2} |z|^{2(\nu+1)} e^{-\frac{z^2+z^{*2}}{8\hat{\alpha}}} \\ \times K_\nu\left(\frac{|z|^2}{4\hat{\alpha}}\right) \eta(z^*)(-)^{\nu+k}(z^*)^{-\nu+k} K_{\nu+k}(z^*)\,. \end{aligned} \tag{4.8}$$

We now deform the y-integration path from the real y-axis to the path shown in figure 1, where $y = y_r + iy_i$ and $\varepsilon \to 0$ after the integration over d^2z. This can be done since the integrand vanishes exponentially for $|y| \to \infty$ along the deformed path and since the integrand has no singularities between the real y-axis and the deformed path. Writing $y = is \mp \varepsilon$ on parts A and C of the path, respectively, we find for eq. (4.8)

$$\begin{aligned}\mathcal{H}_{\nu,k}(\hat{\alpha}, \hat{m}) &= \lim_{\varepsilon \to 0^+} \int_{-\infty}^{\infty} dx \left\{ i \int_{\infty}^{0} ds\, f(x, is - \varepsilon) + \int_{-\varepsilon}^{\varepsilon} dy_r\, f(x, y_r) + i \int_{0}^{\infty} ds\, f(x, is + \varepsilon) \right\} \\ &= \lim_{\varepsilon \to 0^+} i \int_{-\infty}^{\infty} dx \int_{0}^{\infty} ds\, \left[f_+(x, is) - f_-(x, is) \right]\,, \end{aligned} \tag{4.9}$$

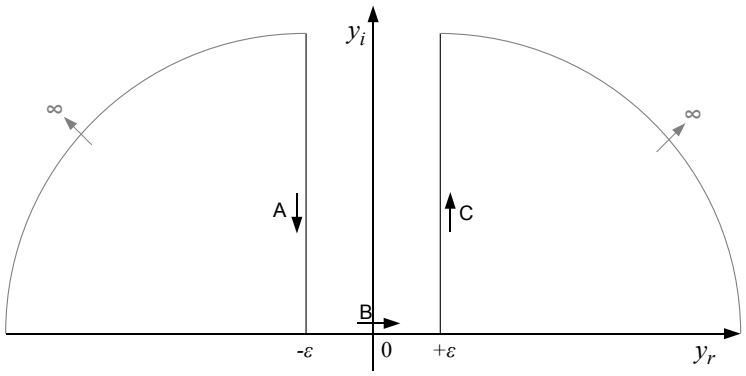

Figure 1. Deformation of the y-integration from the original integration along the y_r-axis to a path on which the integrand vanishes sufficiently rapidly for $|y| \to \infty$.

where we introduced the notation $f_\pm(x, is) = f(x, is \pm \varepsilon)$ with

$$f(x,is) = -\frac{ie^{-2\hat{\alpha}}}{2\pi^2\hat{\alpha}\hat{m}^\nu}\frac{(-)^{\nu+k}(x-s)^{\nu+1}}{(x-s)^2-\hat{m}^2}e^{-\frac{x^2+s^2}{4\hat{\alpha}}} \times K_\nu\left(\frac{x^2-s^2}{4\hat{\alpha}}\right)\eta(x+s)(x+s)^{k+1}K_{\nu+k}(x+s)\,. \tag{4.10}$$

Note that when continuing y to the complex plane we have rewritten the integrand as an explicit function of x and y, since z and z^* are no longer complex conjugate. The second integral in the first line of (4.9) gives zero in the $\varepsilon \to 0$ limit since the integrand is regular at $y = 0$, which is most easily seen by looking back at eq. (3.21). As $\varepsilon \to 0$ in eq. (4.9) we are thus left with the difference of two integrals over semi-infinite sheets infinitesimally close and parallel to the (x, s)-plane, which we denote by S_+ and S_- for $y_r > 0$ and $y_r < 0$, respectively.

The integrand (4.10) can be further simplified by introducing the variable transformation

$$\begin{cases} t = x - s \\ u = x + s \end{cases} \qquad \text{or} \qquad \begin{cases} x = (u+t)/2 \\ s = (u-t)/2 \end{cases} \tag{4.11}$$

with Jacobian 1/2, yielding

$$\mathcal{H}_{\nu,k}(\hat{\alpha},\hat{m}) = \lim_{\varepsilon\to 0^+}\int_{-\infty}^{\infty}dt\int_t^{\infty}du\,[f_+(t,u)+f_-(t,u)]\,, \tag{4.12}$$

where the integration limits in the transformed variables can be read off from figure 2. We introduced the notation $f_\pm(t, u) = f(t_\pm, u_\pm)$ with $t_\pm = x - s \pm i\varepsilon$ and $u_\pm = x + s \mp i\varepsilon$, corresponding to the integrand on the two sheets $S_\pm$. In the transformed variables the integrand is given by

$$f(t,u) = -\frac{e^{-2\hat{\alpha}}}{4\pi^2\hat{\alpha}\hat{m}^\nu}\frac{(-)^{\nu+k}t^{\nu+1}u^{k+1}}{t^2-\hat{m}^2}e^{-\frac{t^2+u^2}{8\hat{\alpha}}}K_\nu\left(\frac{tu}{4\hat{\alpha}}\right)K_{\nu+k}(u)\,, \tag{4.13}$$

JHEP03(2009)100

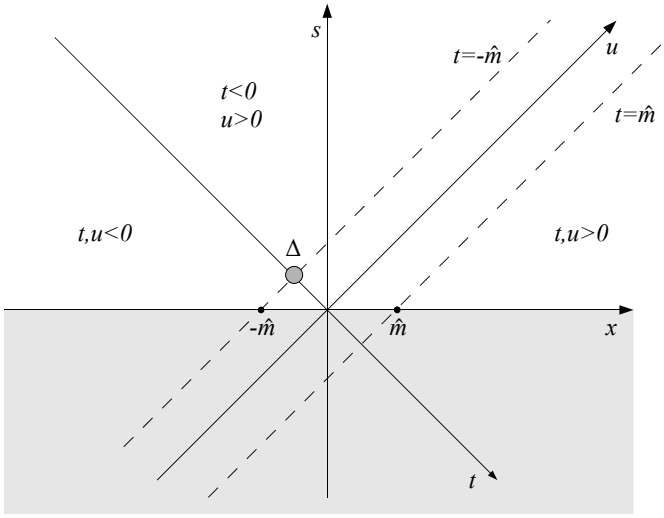

Figure 2. Structure of the integration plane. The integral is computed over the semi-infinite sheets $S_\pm$, with $s > 0$, just above and below the (x, s)-plane. The shaded dot labeled by Δ at $u = 0$, $t = -\hat{m}$ indicates the singularity of the integrand responsible for a new contribution to the phase factor that arises when $\nu \neq 0$.

where we have absorbed the Jacobian and factors of i in the definition of f. We have used $\eta(u_\pm) = \mp 1$ according to eq. (4.5), which changes the difference in eq. (4.9) to a sum in eq. (4.12).

4.3 Singularities of the integrand

When taking the limit $\varepsilon \to 0$ in eq. (4.12) one has to take into account the singularities of the integrand in the (t, u)-plane. There are two mass-pole lines parallel to the u-axis at $t = \pm\hat{m}$ as well as singularities and branch cuts of the K-Bessel functions for zero and negative real argument, respectively (see figure 2).

For future use we first analyze the branch cut of the Bessel functions along the negative real axis. When going from one Riemann sheet to the next across the branch cut, $K_\nu(z)$ changes by $(-)^{\nu+1} 2\pi i I_\nu(z)$ [35, eq. (7.11.45)]. For $x \in \mathbb{R}$ we have

$$\lim_{\varepsilon \to 0^+} K_\nu(x \pm i\varepsilon) = \begin{cases} K_\nu(|x|) & \text{for } x > 0\,, \\ (-)^\nu K_\nu(|x|) \mp i\pi I_\nu(|x|) & \text{for } x < 0\,. \end{cases} \tag{4.14}$$

Consider separately the three sectors of the integration region indicated in figure 2. Using (4.14) together with $t_\pm = t \pm i\varepsilon$, $u_\pm = u \mp i\varepsilon$, and $(tu)_\pm = tu \pm i\varepsilon$ (with $\varepsilon > 0$ because $s > 0$), we can write the product $K_\nu(tu) K_{\nu+k}(u)$ (with the factor $1/4\hat{\alpha}$ omitted

JHEP03(2009)100

for simplicity) appearing in (4.13) as

$$\lim_{\varepsilon\to 0^+}\big[K_\nu(tu)K_{\nu+k}(u)\big]_\pm = \begin{cases} K_\nu(|tu|)K_{\nu+k}(|u|) & \text{for } t,u>0,\\ (-)^\nu K_\nu(|tu|)K_{\nu+k}(|u|) \mp i\pi I_\nu(|tu|)K_{\nu+k}(|u|) & \text{for } t<0<u,\\ (-)^{\nu+k} K_\nu(|tu|)K_{\nu+k}(|u|) \pm i\pi K_\nu(|tu|)I_{\nu+k}(|u|) & \text{for } t,u<0. \end{cases} \tag{4.15}$$

Note that the fourth quadrant, where $t>0$ and $u<0$, does not overlap with the region of integration and thus does not need to be considered.

We now turn to the mass-pole factor in eq. (4.13), which can be written as

$$\frac{1}{(t\pm i\varepsilon)^2-\hat{m}^2} = \frac{1}{2\hat{m}}\left(\frac{1}{t\pm i\varepsilon-\hat{m}} - \frac{1}{t\pm i\varepsilon+\hat{m}}\right). \tag{4.16}$$

This enables us to apply the Sokhatsky-Weierstrass theorem

$$\lim_{\varepsilon\to 0^+}\int_a^b \frac{f(x)}{x\pm i\varepsilon}dx = \mp i\pi f(0) + \mathrm{PV}\int_a^b \frac{f(x)}{x}dx\,, \tag{4.17}$$

where PV denotes the Cauchy principal value integral, to perform the t-integral in eq. (4.12), which thus becomes a sum of the residues at the mass poles $t=\pm\hat{m}$ and a principal value integral over the complete t-axis. In appendix B we show that the principal value part of the t-integral in eq. (4.12) vanishes because of symmetry properties so that the t-integral is entirely determined by the mass-pole contributions. The residue contributions from the mass poles yield two one-dimensional integrals over u along the $t=\pm\hat{m}$ lines, resulting in

$$\begin{aligned}\mathcal{H}_{\nu,k}(\hat{\alpha},\hat{m}) = -\frac{i\pi}{2\hat{m}}\Bigg\{ &\lim_{\varepsilon\to 0^+}\int_{\hat{m}}^\infty du\,[g(\hat{m},u_+)-g(\hat{m},u_-)]\\ &-\lim_{\varepsilon\to 0^+}\int_{-\hat{m}}^\infty du\,[g(-\hat{m},u_+)-g(-\hat{m},u_-)]\Bigg\}, \end{aligned}\tag{4.18}$$

where

$$g(t,u) = (t^2-m^2)f(t,u) = -\frac{e^{-2\hat{\alpha}}}{4\pi^2\hat{\alpha}\hat{m}^\nu}(-)^{\nu+k}t^{\nu+1}u^{k+1}e^{-\frac{t^2+u^2}{8\hat{\alpha}}}K_\nu\left(\frac{tu}{4\hat{\alpha}}\right)K_{\nu+k}(u)\,. \tag{4.19}$$

While the first integral in eq. (4.18) is well-behaved, for $\nu>0$ the integrand of the second integral (for which $t=-\hat{m}$) is singular at $u=0$. This singularity is labeled by Δ in figure 2. To avoid this singularity when taking the $\varepsilon\to 0$ limit, we deform the integration path on $S_\pm$ near zero as shown in figure 3 and then take $\varepsilon\to 0$. This yields

$$\mathcal{H}_{\nu,k}(\hat{\alpha},\hat{m}) = -\frac{i\pi}{2\hat{m}}\left\{\int_{\hat{m}}^\infty du\,G(\hat{m},u) - \lim_{\delta\to 0^+}\left[\int_{-\hat{m}}^{-\delta}+\int_\delta^\infty\right]du\,G(-\hat{m},u)\right\} + \Delta_{\nu,k}(\hat{\alpha},\hat{m}) \tag{4.20}$$

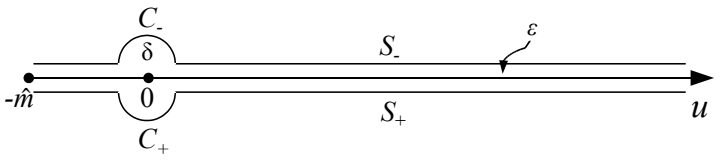

Figure 3. Deformed integration paths over u for $t = -\hat{m}$.

with $G(t,u) = \lim_{\varepsilon\to 0^+}[g(t,u_+) - g(t,u_-)]$. The contribution of the singularity at $u = 0$, which for simplicity will be called the Δ-term, is

$$\Delta_{\nu,k}(\hat{\alpha},\hat{m}) \equiv \frac{i\pi}{2\hat{m}} \lim_{\delta\to 0^+} \left\{ \int_{C_+} du\, g(-\hat{m},u) - \int_{C_-} du\, g(-\hat{m},u) \right\}, \tag{4.21}$$

where $C_\pm$ denotes the two small semicircles shown in figure 3. We shall see in section 4.5 that this term makes a contribution to the phase factor for $\nu \neq 0$.

4.4 Contribution of the branch cut discontinuity

The integrand in the curly braces of eq. (4.20) involves differences that can be simplified using eq. (4.15),

$$\lim_{\varepsilon\to 0^+} \big[K_\nu(tu)K_{\nu+k}(u)\big]_+ - \big[K_\nu(tu)K_{\nu+k}(u)\big]_- = \begin{cases} 0 & \text{for } t,u>0\,, \\ -2i\pi I_\nu(|tu|)K_{\nu+k}(|u|) & \text{for } t<0<u, \\ +2i\pi K_\nu(|tu|)I_{\nu+k}(|u|) & \text{for } t,u<0\,, \end{cases} \tag{4.22}$$

where we have again omitted the factor $1/4\hat{\alpha}$. The only contributions in eq. (4.22) come from the branch cut discontinuity of the K-Bessel function for negative real arguments. The first case in eq. (4.22) vanishes as neither Bessel function has a negative argument and no branch cut discontinuity is encountered. We now use figure 2 to distinguish the various integration regions of eq. (4.20). For the $t = \hat{m}$ integral we always have $t,u > 0$, and according to eq. (4.22) this integral vanishes. Substituting eq. (4.22) in eq. (4.20) with integrand (4.19), we are left with

$$\begin{aligned} \mathcal{H}_{\nu,k}(\hat{\alpha},\hat{m}) = \frac{e^{-2\hat{\alpha}-\frac{\hat{m}^2}{8\hat{\alpha}}}}{4\hat{\alpha}} \Bigg\{ & \int_0^\infty du\,(-)^k u^{k+1} e^{-\frac{u^2}{8\hat{\alpha}}} I_\nu\left(\frac{|\hat{m}u|}{4\hat{\alpha}}\right) K_{\nu+k}(|u|) \\ & + \int_{-\hat{m}}^0 du\,(-)^{k+1} u^{k+1} e^{-\frac{u^2}{8\hat{\alpha}}} K_\nu\left(\frac{|\hat{m}u|}{4\hat{\alpha}}\right) I_{\nu+k}(|u|) \Bigg\} + \Delta_{\nu,k}(\hat{\alpha},\hat{m})\,, \end{aligned} \tag{4.23}$$

where the integration limits $\pm\delta$ in the curly braces of eq. (4.20) were set to zero as the integrands are regular for $u \to 0$. This expression can be simplified by transforming $u \to -u$

in the second integral, and we obtain

$$\mathcal{H}_{\nu,k}(\hat{\alpha},\hat{m}) = \frac{e^{-2\hat{\alpha}-\frac{\hat{m}^2}{8\hat{\alpha}}}}{4\hat{\alpha}} \Bigg\{ \int_0^\infty du\,(-)^k u^{k+1} e^{-\frac{u^2}{8\hat{\alpha}}} I_\nu\left(\frac{\hat{m}u}{4\hat{\alpha}}\right) K_{\nu+k}(u) + \int_0^{\hat{m}} du\, u^{k+1} e^{-\frac{u^2}{8\hat{\alpha}}} K_\nu\left(\frac{\hat{m}u}{4\hat{\alpha}}\right) I_{\nu+k}(u) \Bigg\} + \Delta_{\nu,k}(\hat{\alpha},\hat{m})\,. \quad (4.24)$$

For $\nu = 0$ this expression is identical to the result given previously in ref. [28], as the Δ-term vanishes in this case. For $\nu \neq 0$ the additional contribution is important and will be computed below, see eq. (4.33) for the result. We shall see that it even dominates for small $\hat{m}$.

4.5 Contribution of the Bessel function singularity

The semicircles around the singularity in eq. (4.21) run in opposite directions on the sheets S_+ and S_-. Reversing the direction of integration on one of the sheets changes the difference in eq. (4.21) to a sum.

The K-Bessel functions in the integrand can be split into a meromorphic part with a pole at $u = 0$ and a part containing the branch cut. For $\delta \neq 0$ the integrals along $C_\pm$ would not only receive contributions from the singularity at $u = 0$ but also from the branch cuts, lying on both sides of the origin, which were already included in the line integrals given in eq. (4.24). When $\delta \to 0$ the branch cut contributions will vanish from the integral (4.21), and only the meromorphic part of the integrand will contribute to the Δ-term. Therefore we can rewrite the Δ-term (4.21) as an integral over a closed contour Γ_0 enclosing the singularity of the meromorphic part $\tilde{g}(-\hat{m},u)$ of the integrand. We thus obtain

$$\Delta_{\nu,k}(\hat{\alpha},\hat{m}) = \frac{i\pi}{2\hat{m}} \oint_{\Gamma_0} du\, \tilde{g}(-\hat{m},u)\,, \quad (4.25)$$

where Γ_0 consists of C_+ and C_- and is traversed in the counterclockwise direction.

For $z \to 0$, $K_\nu(z)$ diverges logarithmically for $\nu = 0$ and like $z^{-\nu}$ for $\nu > 0$. Upon multiplication by u^{k+1}, for $\nu = 0$ the integrand (4.19) is not singular at $u = 0$, and thus the Δ-term vanishes in this case. For $\nu > 0$ the integrand has a pole of order $(2\nu - 1)$ at $u = 0$. Using the residue theorem, we obtain

$$\Delta_{\nu,k}(\hat{\alpha},\hat{m}) = \frac{i\pi}{2\hat{m}}\, 2\pi i \operatorname*{Res}_{u=0} \tilde{g} = -\frac{\pi^2}{\hat{m}} a_1\,, \quad (4.26)$$

where a_1 is the coefficient of the u^{-1} term in the Laurent expansion of $\tilde{g}(-\hat{m},u)$ around zero. To find this coefficient, we neglect the u-independent terms in eq. (4.19) and write the u-dependent terms as

$$u f(u) g(u) h(u) = u \underbrace{\exp\Big(-\frac{u^2}{8\hat{\alpha}}\Big)}_{=f} \underbrace{K_\nu\Big(\frac{-\hat{m}u}{4\hat{\alpha}}\Big)}_{=g} \underbrace{\Big[u^k K_{\nu+k}(u)\Big]}_{=h}\,. \quad (4.27)$$

As the product $ug(u)h(u)$ has a singularity of order $2\nu-1$, we need to perform the Taylor expansion of the exponential to order $2\nu-2$ to find all contributions to the simple pole. Hence

$$f(u) \equiv \exp\left(-\frac{u^2}{8\hat{\alpha}}\right) = \sum_{\ell=0}^{\nu-1} \frac{1}{\ell!}\left(-\frac{u^2}{8\hat{\alpha}}\right)^{\ell} + \mathcal{O}\left(u^{2\nu}\right) . \tag{4.28}$$

For $\nu > 0$ the series expansion of $K_\nu(z)$ for small z is [34, eq. (9.6.11)]

$$K_\nu(z) = \frac{2^{\nu-1}}{z^\nu} \sum_{k=0}^{\nu-1} \frac{(\nu-1-k)!}{k!}\left(-\frac{z^2}{4}\right)^k + \mathcal{O}(z^\nu) . \tag{4.29}$$

The functions g and h containing the Bessel functions each need to be expanded to order $\nu-2$ using eq. (4.29), as the remaining part of the integrand is as singular as $u^{1-\nu}$. So

$$g(u) \equiv K_\nu(bu) = \frac{2^{\nu-1}}{(bu)^\nu} \sum_{i=0}^{\nu-1} \frac{(\nu-1-i)!}{i!}\left(-\frac{(bu)^2}{4}\right)^i + \mathcal{O}(u^\nu) \tag{4.30}$$

with $b = -\hat{m}/4\hat{\alpha}$ and

$$h(u) \equiv u^k K_{\nu+k}(u) = \frac{2^{\nu+k-1}}{u^\nu} \sum_{j=0}^{\nu-1} \frac{(\nu+k-1-j)!}{j!}\left(-\frac{u^2}{4}\right)^j + \mathcal{O}(u^\nu) . \tag{4.31}$$

Putting things together yields a triple sum, given by the product of eqs. (4.28), (4.30), and (4.31). Since we are only looking for the coefficient of u^{-1}, we obtain the condition $1+2\ell+(2i-\nu)+(2j-\nu) = -1$, which eliminates one of the sums by setting $\ell = \nu-1-i-j$. Since $\ell \geq 0$ we also have $i+j \leq \nu-1$ and thus

$$\operatorname*{Res}_{u=0}\left[uf(u)g(u)h(u)\right] = -\sum_{i,j=0}^{i+j\leq\nu-1} \frac{(\nu-1-i)!(\nu+k-1-j)!}{(\nu-1-i-j)!i!j!} 2^{\nu+k+1-3i+j}\hat{m}^{-\nu+2i}\hat{\alpha}^{-i+j+1} . \tag{4.32}$$

Combining this expression with the u-independent terms in eq. (4.19) and substituting it in eq. (4.26) yields

$$\Delta_{\nu,k}(\hat{\alpha},\hat{m}) = e^{-2\hat{\alpha}-\frac{\hat{m}^2}{8\hat{\alpha}}} \frac{(-)^k 2^{\nu+k-1}}{\hat{m}^\nu} \sum_{i,j=0}^{i+j\leq\nu-1} \frac{(\nu-1-i)!(\nu+k-1-j)!}{(\nu-1-i-j)!i!j!}\left(\frac{\hat{m}^2}{8\hat{\alpha}}\right)^i (2\hat{\alpha})^j , \tag{4.33}$$

which is a bivariate polynomial of degree $\nu-1$ in $\hat{m}^2/\hat{\alpha}$ and $\hat{\alpha}$ which contains $\nu(\nu+1)/2$

terms. Our final result for $\mathcal{H}_{\nu,k}(\hat{\alpha},\hat{m})$ is thus

$$\begin{aligned}\mathcal{H}_{\nu,k}(\hat{\alpha},\hat{m}) = \frac{e^{-2\hat{\alpha}-\frac{\hat{m}^2}{8\hat{\alpha}}}}{4\hat{\alpha}}\Bigg\{ &\int_0^\infty du\,(-)^k u^{k+1} e^{-\frac{u^2}{8\hat{\alpha}}} I_\nu\left(\frac{\hat{m}u}{4\hat{\alpha}}\right) K_{\nu+k}(u) \\ &+ \int_0^{\hat{m}} du\,u^{k+1} e^{-\frac{u^2}{8\hat{\alpha}}} K_\nu\left(\frac{\hat{m}u}{4\hat{\alpha}}\right) I_{\nu+k}(u)\Bigg\} \\ &+ e^{-2\hat{\alpha}-\frac{\hat{m}^2}{8\hat{\alpha}}}\frac{(-)^k 2^{\nu+k-1}}{\hat{m}^\nu}\sum_{i,j=0}^{i+j\le\nu-1}\frac{(\nu-1-i)!(\nu+k-1-j)!}{(\nu-1-i-j)!i!j!}\left(\frac{\hat{m}^2}{8\hat{\alpha}}\right)^i(2\hat{\alpha})^j\ .\end{aligned} \tag{4.34}$$

As mentioned earlier, for $\nu<0$ one just needs to replace ν by $|\nu|$. Our general expression can also be used for $\nu=0$ as the double sum vanishes and the correct $\nu=0$ result is reproduced.

Note that for $k=0$, eq. (4.34) has been computed in ref. [36] using a different method. The result given in eq. (65) of that reference looks rather different from our result but agrees numerically with eq. (4.34) for $k=0$ after adjusting some prefactors. However, for the calculation of the phase factor using eqs. (3.20) and (3.27) we need the more general result of eq. (4.34) for arbitrary k. The method of ref. [36] does not straightforwardly extend to $k\neq 0$ since it uses orthogonality relations that only hold for $k=0$.

5 Explicit results

5.1 Quenched case

We now write down the explicit form of the phase factor for the quenched case using the solution for the Cauchy transform integral derived in the previous section. Recalling eq. (3.20), we obtain

$$\begin{aligned}\left\langle e_s^{2i\theta}\right\rangle_{N_f=0} = \frac{e^{-2\hat{\alpha}-\frac{\hat{m}^2}{8\hat{\alpha}}}}{4\hat{\alpha}}\Bigg\{ &\int_0^\infty du\,u e^{-\frac{u^2}{8\hat{\alpha}}} I_\nu\left(\frac{\hat{m}u}{4\hat{\alpha}}\right)\left[\hat{m}I_{\nu+1}(\hat{m})K_\nu(u)+I_\nu(\hat{m})uK_{\nu+1}(u)\right] \\ &+ \int_0^{\hat{m}} du\,u e^{-\frac{u^2}{8\hat{\alpha}}} K_\nu\left(\frac{\hat{m}u}{4\hat{\alpha}}\right)\left[\hat{m}I_{\nu+1}(\hat{m})I_\nu(u)-I_\nu(\hat{m})uI_{\nu+1}(u)\right]\Bigg\} \\ &+ \Delta_\nu^{N_f=0}(\hat{\alpha},\hat{m})\,,\end{aligned} \tag{5.1}$$

where

$$\begin{aligned}\Delta_\nu^{N_f=0}(\hat{\alpha},\hat{m}) = e^{-2\hat{\alpha}-\frac{\hat{m}^2}{8\hat{\alpha}}}\frac{2^{\nu-1}}{\hat{m}^\nu}\sum_{i,j=0}^{i+j\le\nu-1}\frac{(\nu-1-i)!(\nu-1-j)!}{(\nu-1-i-j)!i!j!}\left(\frac{\hat{m}^2}{8\hat{\alpha}}\right)^i(2\hat{\alpha})^j \\ \times\begin{vmatrix}1 & -2(\nu-j)\\ I_\nu(\hat{m}) & \hat{m}I_{\nu+1}(\hat{m})\end{vmatrix}\ .\end{aligned} \tag{5.2}$$

The contribution of both terms to the total phase factor will be illustrated in the numerical results of section 5.5.

5.2 One and two dynamical flavors with equal masses

We now give explicit expressions for the one- and two-flavor case. For one dynamical fermion with mass equal to the valence quark mass, the phase factor from eq. (3.29) is given by

$$\left\langle e_s^{2i\theta}\right\rangle_{N_f=1} = \frac{1}{2\hat{m}I_\nu(\hat{m})}\begin{vmatrix} \mathcal{H}_{\nu,0}(\hat{\alpha},\hat{m}) & \mathcal{H}_{\nu,1}(\hat{\alpha},\hat{m}) & \mathcal{H}_{\nu,2}(\hat{\alpha},\hat{m}) \\ I_{\nu,0}(\hat{m}) & I_{\nu,1}(\hat{m}) & I_{\nu,2}(\hat{m}) \\ I'_{\nu,0}(\hat{m}) & I'_{\nu,1}(\hat{m}) & I'_{\nu,2}(\hat{m}) \end{vmatrix}. \tag{5.3}$$

Substituting the solution (4.34) derived in section 4 for the complex integral we find

$$\begin{aligned}\left\langle e_s^{2i\theta}\right\rangle_{N_f=1} = \frac{e^{-2\hat{\alpha}-\frac{\hat{m}^2}{8\hat{\alpha}}}}{8\hat{\alpha}\hat{m}I_\nu(\hat{m})}\Bigg\{ &\int_0^\infty du\, u e^{-\frac{u^2}{8\hat{\alpha}}} I_\nu\left(\frac{\hat{m}u}{4\hat{\alpha}}\right)\begin{vmatrix} K_\nu(u) & -uK_{\nu+1}(u) & u^2K_{\nu+2}(u) \\ I_{\nu,0}(\hat{m}) & I_{\nu,1}(\hat{m}) & I_{\nu,2}(\hat{m}) \\ I'_{\nu,0}(\hat{m}) & I'_{\nu,1}(\hat{m}) & I'_{\nu,2}(\hat{m}) \end{vmatrix} \\ &+ \int_0^{\hat{m}} du\, u e^{-\frac{u^2}{8\hat{\alpha}}} K_\nu\left(\frac{\hat{m}u}{4\hat{\alpha}}\right)\begin{vmatrix} I_\nu(u) & uI_{\nu+1}(u) & u^2I_{\nu+2}(u) \\ I_{\nu,0}(\hat{m}) & I_{\nu,1}(\hat{m}) & I_{\nu,2}(\hat{m}) \\ I'_{\nu,0}(\hat{m}) & I'_{\nu,1}(\hat{m}) & I'_{\nu,2}(\hat{m}) \end{vmatrix}\Bigg\} \\ &+ \frac{2^{\nu-2}e^{-2\hat{\alpha}-\frac{\hat{m}^2}{8\hat{\alpha}}}}{\hat{m}^{\nu+1}I_\nu(\hat{m})}\sum_{i,j=0}^{i+j\le\nu-1}\frac{(\nu-1-i)!(\nu-1-j)!}{(\nu-1-i-j)!i!j!}\left(\frac{\hat{m}^2}{8\hat{\alpha}}\right)^i(2\hat{\alpha})^j \\ &\times\begin{vmatrix} 1 & -2(\nu-j) & 4(\nu-j)_2 \\ I_{\nu,0}(\hat{m}) & I_{\nu,1}(\hat{m}) & I_{\nu,2}(\hat{m}) \\ I'_{\nu,0}(\hat{m}) & I'_{\nu,1}(\hat{m}) & I'_{\nu,2}(\hat{m}) \end{vmatrix}\end{aligned} \tag{5.4}$$

with the Pochhammer symbol $(a)_n$ defined in eq. (C.18). Using $I'_\nu(z) = I_{\nu-1}(z) - \nu I_\nu(z)/z$ [34, eq. (9.6.26)] the derivatives in eq. (5.4) can be explicitly computed,

$$I'_{\nu,k}(\hat{m}) = [\hat{m}^k I_{\nu+k}(\hat{m})]' = \hat{m}^{k-1}\left[\hat{m}I_{\nu+k-1}(\hat{m}) - \nu I_{\nu+k}(\hat{m})\right]. \tag{5.5}$$

For two dynamical fermions with masses equal to that of the valence quark, eq. (3.29) yields

$$\left\langle e_s^{2i\theta}\right\rangle_{N_f=2} = \frac{1}{8\hat{m}^2}\frac{\begin{vmatrix} \mathcal{H}_{\nu,0}(\hat{\alpha},\hat{m}) & \mathcal{H}_{\nu,1}(\hat{\alpha},\hat{m}) & \mathcal{H}_{\nu,2}(\hat{\alpha},\hat{m}) & \mathcal{H}_{\nu,3}(\hat{\alpha},\hat{m}) \\ I_{\nu,0}(\hat{m}) & I_{\nu,1}(\hat{m}) & I_{\nu,2}(\hat{m}) & I_{\nu,3}(\hat{m}) \\ I'_{\nu,0}(\hat{m}) & I'_{\nu,1}(\hat{m}) & I'_{\nu,2}(\hat{m}) & I'_{\nu,3}(\hat{m}) \\ I''_{\nu,0}(\hat{m}) & I''_{\nu,1}(\hat{m}) & I''_{\nu,2}(\hat{m}) & I''_{\nu,3}(\hat{m}) \end{vmatrix}}{\begin{vmatrix} I_{\nu,0}(\hat{m}) & I_{\nu,1}(\hat{m}) \\ I'_{\nu,0}(\hat{m}) & I'_{\nu,1}(\hat{m}) \end{vmatrix}}. \tag{5.6}$$

One can show that

$$\begin{vmatrix} I_{\nu,0}(\hat{m}) & I_{\nu,1}(\hat{m}) \\ I'_{\nu,0}(\hat{m}) & I'_{\nu,1}(\hat{m}) \end{vmatrix} = \hat{m}\left[I_\nu(\hat{m})^2 - I_{\nu-1}(\hat{m})I_{\nu+1}(\hat{m})\right], \tag{5.7}$$

JHEP03(2009)100

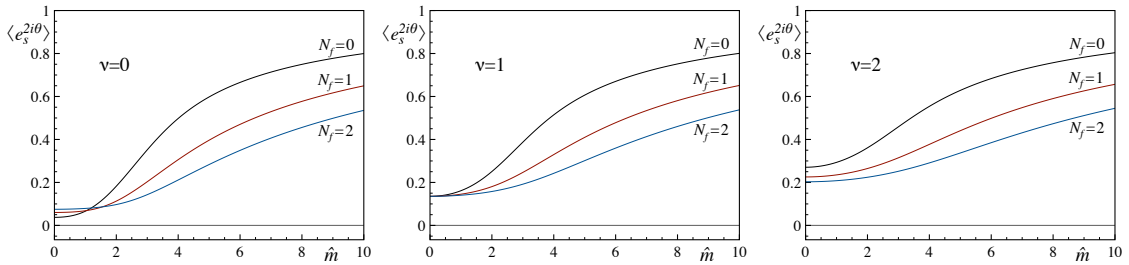

Figure 4. Average phase factor of the fermion determinant for $N_f = 0, 1, 2$ as a function of the fermion mass $\hat{m}$ for $\hat{\alpha} = 1.0$ and $\nu = 0, 1, 2$. We have verified that the $\hat{m} \to 0$ limit of the curves agrees with the chiral limit computed analytically in section 5.3.

and using the solution (4.34) for the complex integral we find

$$\begin{aligned}
\left\langle e_s^{2i\theta}\right\rangle_{N_f=2} = & \frac{e^{-2\hat{\alpha}-\frac{\hat{m}^2}{8\hat{\alpha}}}}{32\hat{\alpha}\hat{m}^3\left[I_\nu(\hat{m})^2 - I_{\nu-1}(\hat{m})I_{\nu+1}(\hat{m})\right]} \\
& \times \left\{ \int_0^\infty du\, u e^{-\frac{u^2}{8\hat{\alpha}}} I_\nu\left(\frac{\hat{m}u}{4\hat{\alpha}}\right) \begin{vmatrix} K_\nu(u) & -uK_{\nu+1}(u) & u^2K_{\nu+2}(u) & -u^3K_{\nu+3}(u) \\ I_{\nu,0}(\hat{m}) & I_{\nu,1}(\hat{m}) & I_{\nu,2}(\hat{m}) & I_{\nu,3}(\hat{m}) \\ I'_{\nu,0}(\hat{m}) & I'_{\nu,1}(\hat{m}) & I'_{\nu,2}(\hat{m}) & I'_{\nu,3}(\hat{m}) \\ I''_{\nu,0}(\hat{m}) & I''_{\nu,1}(\hat{m}) & I''_{\nu,2}(\hat{m}) & I''_{\nu,3}(\hat{m}) \end{vmatrix} \right. \\
& \left. + \int_0^{\hat{m}} du\, u e^{-\frac{u^2}{8\hat{\alpha}}} K_\nu\left(\frac{\hat{m}u}{4\hat{\alpha}}\right) \begin{vmatrix} I_\nu(u) & uI_{\nu+1}(u) & u^2I_{\nu+2}(u) & u^3I_{\nu+3}(u) \\ I_{\nu,0}(\hat{m}) & I_{\nu,1}(\hat{m}) & I_{\nu,2}(\hat{m}) & I_{\nu,3}(\hat{m}) \\ I'_{\nu,0}(\hat{m}) & I'_{\nu,1}(\hat{m}) & I'_{\nu,2}(\hat{m}) & I'_{\nu,3}(\hat{m}) \\ I''_{\nu,0}(\hat{m}) & I''_{\nu,1}(\hat{m}) & I''_{\nu,2}(\hat{m}) & I''_{\nu,3}(\hat{m}) \end{vmatrix} \right\} \\
& + \frac{2^{\nu-4}e^{-2\hat{\alpha}-\frac{\hat{m}^2}{8\hat{\alpha}}}}{\hat{m}^{\nu+3}\left[I_\nu(\hat{m})^2 - I_{\nu-1}(\hat{m})I_{\nu+1}(\hat{m})\right]} \sum_{i,j=0}^{i+j\le\nu-1} \frac{(\nu-1-i)!(\nu-1-j)!}{(\nu-1-i-j)!i!j!} \left(\frac{\hat{m}^2}{8\hat{\alpha}}\right)^i \\
& \times (2\hat{\alpha})^j \begin{vmatrix} 1 & -2(\nu-j) & 4(\nu-j)_2 & -8(\nu-j)_3 \\ I_{\nu,0}(\hat{m}) & I_{\nu,1}(\hat{m}) & I_{\nu,2}(\hat{m}) & I_{\nu,3}(\hat{m}) \\ I'_{\nu,0}(\hat{m}) & I'_{\nu,1}(\hat{m}) & I'_{\nu,2}(\hat{m}) & I'_{\nu,3}(\hat{m}) \\ I''_{\nu,0}(\hat{m}) & I''_{\nu,1}(\hat{m}) & I''_{\nu,2}(\hat{m}) & I''_{\nu,3}(\hat{m}) \end{vmatrix}
\end{aligned} \tag{5.8}$$

with the Pochhammer symbol $(a)_n$ from eq. (C.18).

In figure 4 we compare the mass dependence of the average phase factor in the quenched case, given by eq. (5.1), with the predictions for one and two dynamical flavors from eqs. (5.4) and (5.8). Although the sign problem becomes less severe as the fermion mass increases, the dynamical quarks have a negative effect as they clearly reduce the value of the phase factor. Note that, surprisingly, for $\nu = 0$ and small mass ($\hat{m} \lesssim 1$) the effect of the dynamical quarks seems to be reversed (this is true for any value of $\hat{\alpha}$). This is related to the fact that for $\nu = 1$ the chiral limit of the average phase factor is equal to $e^{-2\hat{\alpha}}$, independently of the number of flavors, see eq. (5.10) below. This is also verified in the middle plot of figure 4.

JHEP03(2009)100

5.3 Chiral limit

In the limit $\hat{m} \to 0$ the phase factor (3.30) can be simplified and written in terms of special functions. The limit has to be derived differently for $\nu = 0$ and for $\nu \neq 0$, and the general derivation for arbitrary N_f can be found in appendix C. For trivial topology the result is given by eq. (C.15),

$$\langle e_s^{2i\theta} \rangle_{\nu=0,\hat{m}=0} = (N_f+1)(2\hat{\alpha})^{N_f+1}\Gamma(-N_f-1, 2\hat{\alpha}) \,, \tag{5.9}$$

where $\Gamma(a,z)$ is the incomplete gamma function. For nontrivial topology the result is given by eq. (C.17),

$$\langle e_s^{2i\theta} \rangle_{\nu>0,\hat{m}=0} = e^{-2\hat{\alpha}} \sum_{j=0}^{\nu-1} \frac{(\nu-j)_{N_f+1}}{(\nu)_{N_f+1}} \frac{(2\hat{\alpha})^j}{j!} \,, \tag{5.10}$$

where the Pochhammer symbol $(a)_n$ is defined in eq. (C.18). Note that for $\nu = 1$ the phase factor is simply given by $e^{-2\hat{\alpha}}$, independently of N_f. The result (5.10) can also be expressed in terms of incomplete gamma functions as shown in eq. (C.25),

$$\langle e_s^{2i\theta} \rangle_{\hat{m}=0} = \frac{1}{(\nu+N_f)!} \sum_{k=0}^{N_f+1} (-)^k \binom{N_f+1}{k} (\nu-k)_{N_f+1} (2\hat{\alpha})^k \Gamma(\nu-k, 2\hat{\alpha}) \,. \tag{5.11}$$

The last expression is also valid for $\nu = 0$, see eq. (C.26). The quenched results are obtained by setting $N_f = 0$ in the above equations.

As discussed in appendix C, for $\hat{m} = 0$ and $\nu \neq 0$ the phase of the determinant is exclusively given by the new Δ-term. It is interesting to note that the contributions to the phase of the determinant in the chiral limit originate from different terms for $\nu = 0$ and $\nu \neq 0$.

5.4 Thermodynamic limit

The thermodynamic limit of the phase factor (3.30) is the limit of that equation for $\hat{\alpha} = \mu^2 F^2 V \to \infty$ and $\hat{m} = mV\Sigma \to \infty$. As discussed in ref. [28], this limit depends on whether $2\hat{\alpha}/\hat{m}$ (or, equivalently, $2\mu/m_\pi$) is smaller or larger than 1. We find that for $2\hat{\alpha} < \hat{m}$ the thermodynamic limit is given by

$$\langle e_s^{2i\theta} \rangle^{\text{th}} = (1 - 2\hat{\alpha}/\hat{m})^{N_f+1} \,. \tag{5.12}$$

As expected, the thermodynamic limit does not depend on ν, which is a consistency check of our result. Equation (5.12) agrees with the special cases $\nu = 0$ and $N_f = 0, 1, 2$ considered in ref. [28]. The proof of our general result is given in appendix D. Note that the contribution of the Δ-term vanishes in the thermodynamic limit. For $2\hat{\alpha} > \hat{m}$ the phase factor is exponentially suppressed in the volume so that its thermodynamic limit is zero. An asymptotic large-volume expansion of the phase factor could be computed for this case from eq. (3.30), analogously to ref. [28].

In figure 5 we show how the thermodynamic limit is approached for the case of $N_f = 2$ and $\nu = 2$.

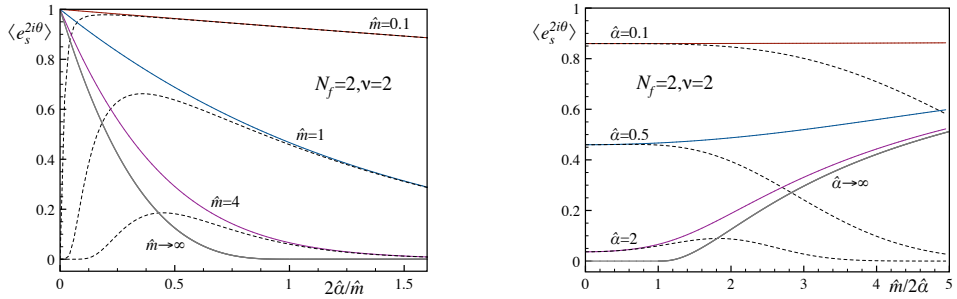

Figure 5. The left plot shows how the $\hat{\alpha}$-dependence of the phase factor changes as a function of $\hat{m}$. In the right plot the roles of $\hat{\alpha}$ and $\hat{m}$ are reversed. The curves $\hat{m} \to \infty$ and $\hat{\alpha} \to \infty$ correspond to the thermodynamic limit (5.12). The dashed lines indicate the contribution of the Δ-term to the phase factor (this contribution vanishes in the thermodynamic limit).

5.5 Numerical simulations

To check our analytical results and especially the contribution of the Δ-term, which is new in the $\nu \neq 0$ case, we performed numerical random matrix simulations to compute the average phase factor of the fermion determinant in quenched chRMT. The simulation details can be found in appendix E.

In order to keep the statistical error sufficiently small the simulations were performed with samples of 100,000 random matrices. Figure 6 shows the $\hat{\alpha}$-dependence of the quenched average phase factor for $\nu = 0, 1, 2, 3, 4, 5$ with $\hat{m} = 0$ and matrix size $N = 20$. The simulation results are compared with the chiral limit of the analytical results given in eqs. (5.9) and (5.10) with $N_f = 0$. The agreement is extremely good except for larger values of ν (≥ 3) where the simulation results lie slightly, but systematically, below the predictions. This is merely a finite-N effect, which is also clear from the comparison with the exact finite-N result shown for $\nu = 5$. The convergence towards the microscopic limit is illustrated in figure 7, where we show the N-dependence of the average phase factor for two typical cases: fast convergence for $\hat{\alpha} = 0.22$, $\nu = 2$ versus slow convergence for $\hat{\alpha} = 2$, $\nu = 4$. The figure can help us determine how large the random matrices need to be in order to reproduce the analytical results in the $N \to \infty$ limit. In the figure we also show the N-dependence of the phase factor from the theoretical framework, by numerically solving the two-dimensional integral for the finite-N expression (3.7), which is expressed in terms of generalized Laguerre polynomials. We find perfect agreement with the data of figure 7, within statistical errors, for N from 1 to about 30, at which point the integrals oscillate too strongly, prohibiting Mathematica from performing the numerical integration with sufficient accuracy.

From the study of the N-dependence we conclude that for $\nu = 0, 1, 2$ it suffices to take $N = 20$. However, for $\nu = 3, 4, 5$ we increased the matrix size to $N = 80$ to be close enough to the microscopic limit. As can be seen in figure 8, this increase in N results in excellent agreement between simulations and analytical predictions for larger ν as well. Note that the $\hat{m} = 0$ case is a key test for the new $\nu \neq 0$ contribution (5.2), as only this term contributes in the chiral limit. From figures 6 and 8 we conclude that, as expected,

JHEP03(2009)100

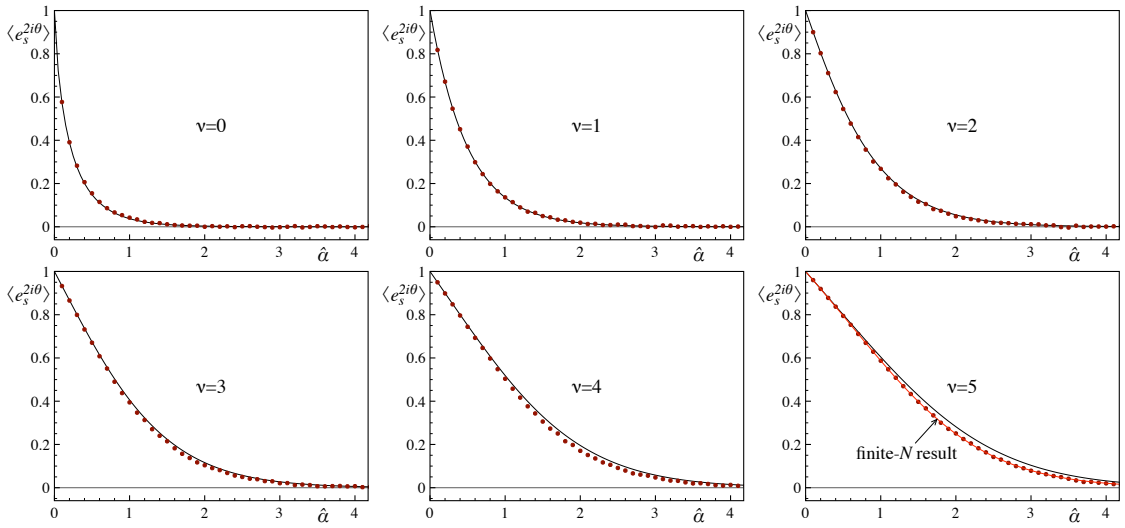

Figure 6. Average phase factor of the fermion determinant with $\hat{m} = 0$ in the quenched case for varying chemical potential parameter $\hat{\alpha}$ and $\nu = 0, 1, 2, 3, 4, 5$. The full lines are the predictions of eqs. (5.9) and (5.10) for $N_f = 0$. For $\nu = 5$ we also show the exact finite-N result from eq. (3.7). The data points were computed from RMT simulations with matrix size $N = 20$ and 100,000 samples. No error bars are shown since they are smaller than the data points.

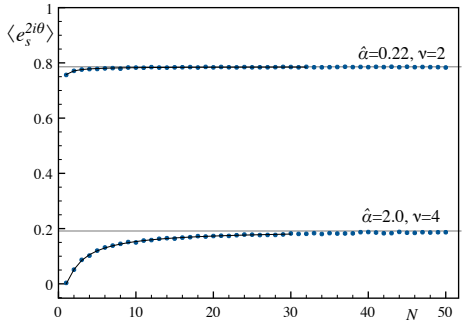

Figure 7. Average phase factor vs matrix size N. The horizontal lines show the analytical predictions in the microscopic limit ($N \to \infty$), while the solid lines going through the data points are the finite-N results from eq. (3.7) for $N \leq 30$. The upper curve was computed with $\hat{\alpha} = 0.22$, $\nu = 2$, the lower with $\hat{\alpha} = 2$, $\nu = 4$, both for $N_f = 0$ and $\hat{m} = 0$.

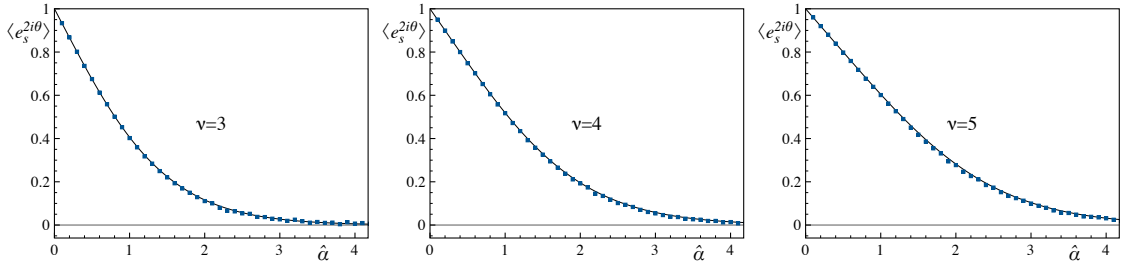

Figure 8. Average phase factor of the fermion determinant as a function of the chemical potential parameter $\hat{\alpha}$ for $\nu = 3, 4, 5$ with $N_f = 0$ and $\hat{m} = 0$ as in figure 6, but with increased $N = 80$.

JHEP03(2009)100

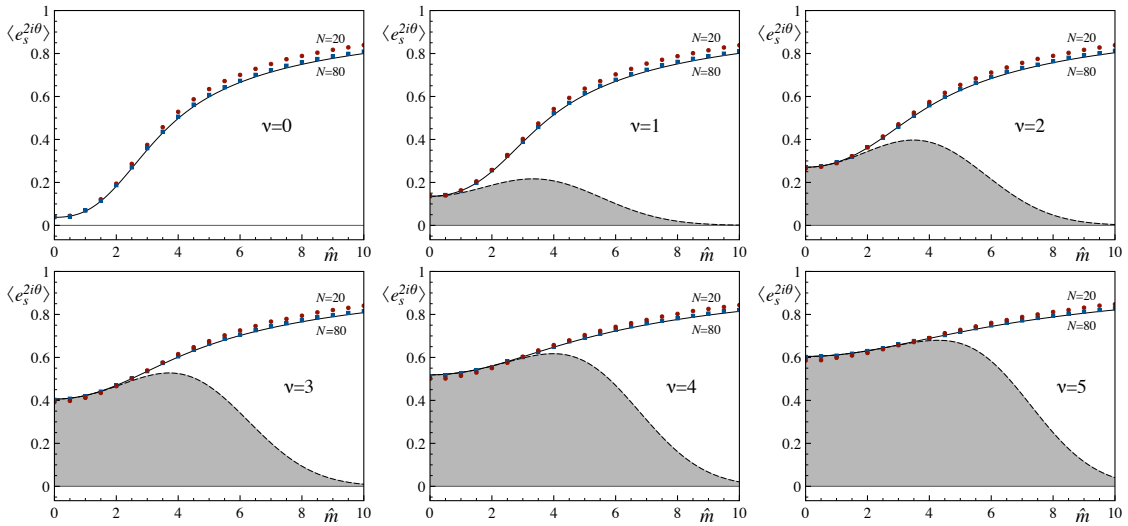

Figure 9. Average phase factor of the fermion determinant as a function of the fermion mass $\hat{m}$ for $N_f = 0$, $\hat{\alpha} = 1.0$, and $\nu = 0, 1, 2, 3, 4, 5$. The simulations were performed with $N = 20$ (red points) and $N = 80$ (blue squares). The latter data are already very close to the RMT-predictions for $N \to \infty$ (full lines). The filled area shows the contribution of the Δ-term specific to $\nu \neq 0$. (Note that we generated different random samples for each $\hat{m}$ to avoid misleading correlations between measurements.)

the average phase factor becomes unity when the chemical potential vanishes, as the Dirac operator then becomes anti-Hermitian and the determinant real. For large $\hat{\alpha}$ the average phase factor goes to zero, pointing to the increasing sign problem in dynamical simulations at large chemical potential. Observe that for increasing topology the sign problem seems to be delayed, as it sets in at a larger value of the chemical potential.

In figure 9 we verify the mass-dependence of the analytical formula (5.1) and compare its predictions with the results from random matrix simulations as a function of $\hat{m}$ for fixed $\hat{\alpha}$. Note that the convergence to the microscopic limit slows down as the mass increases. This is noticeable in figure 9, where the $N = 20$ data (red points) show a systematic deviation from the RMT-predictions. When increasing the size to $N = 80$ (blue squares) the agreement improves substantially. The importance of the new Δ-term for $\nu \neq 0$ is highlighted in figure 9 by the gray area, which corresponds to the contribution of the Δ-term in eq. (5.1). This clearly shows how this term dominates for small masses. We also observe in figure 9 that for fixed $\hat{m}$ and $\hat{\alpha}$ the sign problem becomes less severe as the topological charge is increased.

Figures 6–9 demonstrate that the numerical simulations confirm the analytical prediction (5.1) for general topology in the quenched case. We are currently investigating the implementation of unquenched random matrix simulations at nonzero chemical potential using the analytical information we have obtained about the sign problem.

JHEP03(2009)100

6 Conclusions

Dynamical lattice simulations of QCD at nonzero baryon density are plagued by the sign problem caused by the oscillating fermion determinant. To investigate this problem it is helpful to employ the equivalence between chiral perturbation theory in the ε-regime of QCD and chiral random matrix theory, which also holds at nonzero chemical potential. As the average phase factor of the fermion determinant is an important clue in the study of the sign problem, it is a valuable quantity to compute in the framework of chiral random matrix theory.

In this paper we derived an analytical formula for the average phase factor of the fermion determinant in quenched and unquenched chiral random matrix theory for general topology. The formula is a nontrivial extension of the result previously published by Splittorff and Verbaarschot for zero topology [28]. For nonzero topology a new contribution shows up, which dominates the phase factor for small valence quark mass. The new formula suggests that the severity of the sign problem is reduced as the topological charge increases. We also computed the chiral and thermodynamic limits from our general formula.

The quenched formula was verified by random matrix simulations in different regimes of mass and chemical potential and for different values of the topological charge. Excellent agreement was found between theory and simulations. We are currently in the process of comparing the RMT predictions derived in this paper to lattice QCD data computed with the overlap operator at nonzero chemical potential.

Acknowledgments

This work was supported in part by DFG grant FOR465-WE2332/4-2. JB would like to thank G. Akemann for his hospitality and helpful suggestions on a visit to Brunel University. TW would like to thank the Theory Group of the INPS at KEK Tsukuba, where part of this work was carried out, for their hospitality and support. We would also like to thank T. Kaltenbrunner and C. Lehner for motivating discussions.

A Microscopic limit of the orthogonal polynomials

In this section we define and compute the microscopic limits of the orthogonal polynomials (2.9), the normalization factor (2.11), and the weight function (2.7).

The microscopic limit of the orthogonal polynomials (2.9) is defined as

$$\begin{aligned} p_s^\nu(\hat{z};\hat{\alpha}) &\equiv \lim_{N\to\infty} \frac{e^N}{(2N)^{\nu+1/2}} p_{N-1}^\nu(\hat{z}/2N;\hat{\alpha}/2N) \\ &= \lim_{N\to\infty} \frac{e^N}{(2N)^{\nu+1/2}} \left(1-\frac{\hat{\alpha}}{2N}\right)^{N-1} \frac{(N-1)!}{N^{N-1}} L_{N-1}^\nu\left(-\frac{\hat{z}^2}{4N}\right) . \end{aligned} \tag{A.1}$$

Using the definition of the exponential function,

$$\lim_{N\to\infty} \left(1-\frac{\hat{\alpha}}{2N}\right)^{N-1} = e^{-\hat{\alpha}/2} , \tag{A.2}$$

and Stirling's formula, from which we obtain

$$\frac{(N-1)!}{N^{N-1}} = \frac{N!}{N^N} \overset{N\to\infty}{\longrightarrow} \sqrt{2\pi N} e^{-N} \,, \tag{A.3}$$

we find

$$p_s^\nu(\hat{z};\hat{\alpha}) = \lim_{N\to\infty} \sqrt{\pi} e^{-\hat{\alpha}/2} (2N)^{-\nu} L_{N-1}^\nu \left(-\frac{\hat{z}^2}{4N}\right) \,. \tag{A.4}$$

The $N \to \infty$ limit of the Laguerre polynomial in eq. (A.4) is given by [37, eq. (8.982.2)]

$$\lim_{N\to\infty} N^{-\nu} L_N^\nu \left(-\frac{z^2}{4N}\right) = 2^\nu z^{-\nu} I_\nu(z) \,, \tag{A.5}$$

and hence eq. (A.4) becomes

$$p_s^\nu(\hat{z};\hat{\alpha}) = \sqrt{\pi} e^{-\hat{\alpha}/2} \hat{z}^{-\nu} I_\nu(\hat{z}) \,. \tag{A.6}$$

Next, the microscopic limit of the normalization factor (2.11) is defined as

$$\begin{aligned} r_s^\nu(\hat{\alpha}) &\equiv \lim_{N\to\infty} (2N)^2 e^{2N} r_{N-1}^\nu(\hat{\alpha}/2N) \\ &= \lim_{N\to\infty} \frac{(2N)^2 e^{2N}}{N^{2N+\nu}} \pi \frac{\hat{\alpha}}{2N} \left(1+\frac{\hat{\alpha}}{2N}\right)^{2N-2+\nu} (N-1)!(N-1+\nu)! \\ &= 4\pi^2 \hat{\alpha} e^{\hat{\alpha}} \,, \end{aligned} \tag{A.7}$$

where we again used eqs. (A.2) and (A.3). Finally, the microscopic limit of the weight function (2.7) is defined as

$$\begin{aligned} w_s^\nu(\hat{z},\hat{z}^*;\hat{\alpha}) &= \lim_{N\to\infty} (2N)^{2\nu+2} w^\nu(\hat{z}/2N, \hat{z}^*/2N; \hat{\alpha}/2N) \\ &= \lim_{N\to\infty} |\hat{z}|^{2(\nu+1)} \exp\left(-\frac{N(1-\hat{\alpha}/2N)}{4\hat{\alpha}/2N} \frac{\hat{z}^2+\hat{z}^{*2}}{4N^2}\right) K_\nu\left(\frac{N(1+\hat{\alpha}/2N)}{2\hat{\alpha}/2N} \frac{|\hat{z}|^2}{4N^2}\right) \\ &= |\hat{z}|^{2(\nu+1)} \exp\left(-\frac{\hat{z}^2+\hat{z}^{*2}}{8\hat{\alpha}}\right) K_\nu\left(\frac{|\hat{z}|^2}{4\hat{\alpha}}\right) \,. \end{aligned} \tag{A.8}$$

B Principal value integral

In this section we show that the principal value integral originating from the application of the Sokhatsky-Weierstrass theorem (4.17) to eq. (4.12) vanishes because of symmetry considerations.

For $\nu > 0$, the integrand (4.13) of the principal value integral over t is singular along the line $u = 0$ (for which $t < 0$ in the integration region). Therefore we split the u-integral into a principal value part and a line integral circumventing the singularity of the Bessel functions at $u = 0$. (To simplify the notation we do this also for $\nu = 0$ even though there is no singularity in this case.) For any $t < 0$, the u-integration in eq. (4.12) is thus rewritten as

$$\int_t^\infty du f_\pm(t,u) = \lim_{\delta\to 0^+} \left\{ \int_t^{-\delta} + \int_{C_\pm} + \int_\delta^\infty \right\} du\, f_\pm(t,u) \,, \tag{B.1}$$

where $C_\pm$ denotes the small semicircles shown in figure 3. The principal value integral over t in eq. (4.12) therefore becomes

$$\begin{aligned}\mathrm{PV}_t \int_{-\infty}^{\infty} dt \lim_{\varepsilon\to 0^+} \int_t^{\infty} du\,[f_+(t,u)+f_-(t,u)] = \\ \mathrm{PV}_{tu} \int_{-\infty}^{\infty} dt \int_t^{\infty} du\, F(t,u) \\ + \mathrm{PV}_t \int_{-\infty}^{0} dt \lim_{\delta\to 0^+} \left\{ \int_{C_+} du\, f_+(t,u) + \int_{C_-} du\, f_-(t,u) \right\},\end{aligned} \tag{B.2}$$

where $F(t,u) = \lim_{\varepsilon\to 0^+}[f_+(t,u)+f_-(t,u)]$. The total principal value integral PV_{tu} can be split, for any t, as

$$\mathrm{PV}_{tu} \int_{-\infty}^{\infty} dt \int_t^{\infty} du\, F(t,u) = \underbrace{\mathrm{PV}_{tu} \int_{-\infty}^{\infty} dt \int_0^{\infty} du\, F(t,u)}_{=A} + \underbrace{\mathrm{PV}_{tu} \int_{-\infty}^{\infty} dt \int_t^{0} du\, F(t,u)}_{=B}\,. \tag{B.3}$$

From eq. (4.13) we see that the dependence of the integrand on t and u is given by

$$f(t,u) \propto \frac{t^{\nu+1}u^{k+1}}{t^2-\hat{m}^2} e^{-\frac{t^2+u^2}{8\hat{\alpha}}} K_\nu\left(\frac{tu}{4\hat{\alpha}}\right) K_{\nu+k}(u)\,, \tag{B.4}$$

and according to eq. (4.15) the sum of the contributions on the upper and lower sheets, S_+ and S_-, is proportional to (again with the factor $1/4\hat{\alpha}$ omitted)

$$\lim_{\varepsilon\to 0^+} \big[K_\nu(tu)K_{\nu+k}(u)\big]_+ + \big[K_\nu(tu)K_{\nu+k}(u)\big]_- = \begin{cases} 2K_\nu(|tu|)K_{\nu+k}(|u|) & \text{for } t,u>0, \\ 2(-)^\nu K_\nu(|tu|)K_{\nu+k}(|u|) & \text{for } t<0<u, \\ 2(-)^{\nu+k} K_\nu(|tu|)K_{\nu+k}(|u|) & \text{for } t,u<0. \end{cases} \tag{B.5}$$

From eqs. (B.4) and (B.5) we see that the integrand of A in eq. (B.3) is odd in t, and hence the principal value of that integral vanishes. Integral B of eq. (B.3) can be rewritten as

$$\begin{aligned}\mathrm{PV}_{tu} \int_{-\infty}^{\infty} dt \int_t^{0} du\, F(t,u) &= \mathrm{PV}_{tu} \left\{ \int_{-\infty}^{0} dt \int_t^{0} du\, F(t,u) - \int_0^{\infty} dt \int_0^{t} du\, F(t,u) \right\} \\ &= \mathrm{PV}_{tu} \left\{ \int_0^{\infty} dt \int_0^{t} du\, F(-t,-u) - \int_0^{\infty} dt \int_0^{t} du\, F(t,u) \right\}.\end{aligned} \tag{B.6}$$

From eqs. (B.4) and (B.5) we find for $u,t>0$

$$F(-t,-u) = (-)^{\nu+1}(-)^{k+1}(-)^{\nu+k} F(t,u) = F(t,u)\,, \tag{B.7}$$

and hence (B.6) and the total principal value integral (B.3) vanish because of symmetry considerations.

JHEP03(2009)100

Next we treat the last term in eq. (B.2). For $\nu = 0$ the integrand (B.4) is regular at $u = 0$, and thus the integral trivially vanishes as $\delta \to 0$. For $\nu > 0$ one can expand the integrand in pole terms behaving like

$$u^{-2(\nu-j)+1}\,, \qquad j = 0, \ldots, \nu - 1 \tag{B.8}$$

for $u \to 0$ by using the small-argument expansion (4.29) of the K-Bessel functions. The u-integration around the pole flows in opposite directions for the integration on the lower and upper sheet. The simple pole gives contributions with opposite signs on the two sheets so that their sum is zero. The higher-order poles of the integrand are also odd in u, and one can show that the integrals along C_+ and C_- vanish individually, so that

$$\mathrm{PV}_t \int_{-\infty}^{0} dt \lim_{\delta\to 0^+} \left\{ \int_{C_+} du\, f_+(t,u) + \int_{C_-} du\, f_-(t,u) \right\} = 0\,. \tag{B.9}$$

This completes the proof that the integral (B.2) vanishes.

C Chiral limit

In the limit $\hat{m} \to 0$ the phase factor can be simplified and written in terms of special functions. Our starting point is eq. (3.30), and we need to compute the chiral limit of the Wronskian (3.32), which contains the function $I_{\nu,k}$ defined in eq. (3.23). For small argument $\hat{m}$ the leading order term of the I-Bessel function is [34, eq. (9.6.10)]

$$I_\nu(\hat{m}) \sim \frac{\hat{m}^\nu}{2^\nu \nu!}\,, \tag{C.1}$$

from which we obtain

$$I_{\nu,k}(\hat{m}) \sim \frac{\hat{m}^{\nu+2k}}{2^{\nu+k}(\nu+k)!} \tag{C.2}$$

and its p-th derivative

$$I^{(p)}_{\nu,k}(\hat{m}) \sim \frac{(\nu+2k)!}{2^{\nu+k}(\nu+k)!(\nu+2k-p)!}\hat{m}^{\nu+2k-p}\,. \tag{C.3}$$

Substituting these expressions in the Wronskian (3.32) and using properties of the determinant gives the leading-order result

$$W_n(k_1,\ldots,k_n) \sim \frac{\hat{m}^{n\nu+2\sum_i k_i - n(n-1)/2}}{2^{n\nu+\sum_i k_i - n(n-1)/2}\prod_i(\nu+k_i)!}\Delta_n(k_1,\ldots,k_n)\,, \tag{C.4}$$

where $\Delta_n(k_1,\ldots,k_n)$ is a Vandermonde determinant. From this we compute the chiral limit of the denominator in eq. (3.30),

$$W_{N_f}(0,1,\ldots,N_f-1) \sim \frac{\hat{m}^{N_f\nu+N_f(N_f-1)/2}}{2^{N_f\nu}\prod_{i=0}^{N_f-1}(\nu+i)!}\prod_{\ell=1}^{N_f-1}\ell!\,, \tag{C.5}$$

where we used the identities

$$\Delta_{N_f}(0,1,\ldots,N_f-1)=\prod_{\ell=1}^{N_f-1}\ell!\quad\text{and}\quad\sum_{i=0}^{N_f-1}i=\frac{1}{2}N_f(N_f-1)\,. \tag{C.6}$$

From eq. (C.4) it is easy to see that in the limit $\hat{m}\to 0$ only the Wronskian corresponding to the $k=N_f+1$ term in eq. (3.31) will contribute to leading order, while all other terms will be of higher order. The phase factor (3.30) can therefore be written as

$$\left\langle e_s^{2i\theta}\right\rangle_{\hat{m}=0}=\lim_{\hat{m}\to 0}\frac{(-)^{N_f+1}}{(2\hat{m})^{N_f}N_f!}\frac{W_{N_f+1}(0,1,\ldots,N_f)}{W_{N_f}(0,1,\ldots,N_f-1)}\mathcal{H}_{\nu,N_f+1}(\hat{\alpha},\hat{m})\,. \tag{C.7}$$

After substituting (C.5) we find

$$\left\langle e_s^{2i\theta}\right\rangle_{\hat{m}=0}=\frac{(-)^{N_f+1}}{2^{\nu+N_f}(\nu+N_f)!}\lim_{\hat{m}\to 0}\hat{m}^{\nu}\mathcal{H}_{\nu,N_f+1}(\hat{\alpha},\hat{m})\,. \tag{C.8}$$

The chiral limit of $\mathcal{H}_{\nu,k}(\hat{\alpha},\hat{m})$ has to be derived differently for $\nu=0$ and for $\nu\neq 0$. For $\nu=0$ and $\hat{m}\to 0$ only the first integral in eq. (4.34) contributes as the Δ-term is absent and the second integral vanishes because the integration range is empty. Hence,

$$\mathcal{H}_{0,k}(\hat{\alpha},0)=\frac{e^{-2\hat{\alpha}}}{4\hat{\alpha}}\int_0^\infty du\,(-)^k u^{k+1}e^{-\frac{u^2}{8\hat{\alpha}}}K_k(u)\,. \tag{C.9}$$

The integral in eq. (C.9) can be evaluated analytically in terms of an incomplete gamma function. Assuming that n is a nonnegative integer and $\operatorname{Re} z>0$, we find from ref. [37, eq. (6.631.3)]

$$\mathcal{I}_n(z)\equiv\int_0^\infty du\,u^{n+1}e^{-\frac{u^2}{4z}}K_n(u)=2^n n!\,z^{\frac{n+1}{2}}e^{z/2}W_{-\frac{n+1}{2},\frac{n}{2}}(z)\,, \tag{C.10}$$

where $W_{\lambda,\mu}$ is a Whittaker function with integral representation [37, Erratum of eq. (9.222.1)]

$$W_{\lambda,\mu}(z)=\frac{z^{\mu+\frac{1}{2}}e^{-z/2}}{\Gamma(\mu-\lambda+\frac{1}{2})}\int_0^\infty dt\,e^{-zt}t^{\mu-\lambda-\frac{1}{2}}(1+t)^{\mu+\lambda-\frac{1}{2}}\,. \tag{C.11}$$

Setting $\lambda=-(n+1)/2$ and $\mu=n/2$ in this equation and substituting in eq. (C.10) gives

$$\mathcal{I}_n(z)=2^n z^{n+1}\int_0^\infty dt\,e^{-zt}\frac{t^n}{1+t}=2^n z^{n+1}n!e^z\Gamma(-n,z)\,, \tag{C.12}$$

where the last equality follows from [37, eq. (3.383.10)] and the incomplete gamma function is given by

$$\Gamma(a,z)=\int_z^\infty dt\,t^{a-1}e^{-t}\,. \tag{C.13}$$

After substituting the integral (C.12) in eq. (C.9) we find

$$\mathcal{H}_{0,k}(\hat{\alpha},0)=(-)^k 2^{k-1}k!(2\hat{\alpha})^k\Gamma(-k,2\hat{\alpha})\,. \tag{C.14}$$

JHEP03(2009)100

Substituting the latter in eq. (C.8) with $\nu = 0$ yields

$$\left\langle e_s^{2i\theta} \right\rangle_{\nu=0,\hat{m}=0} = (N_f+1)(2\hat{\alpha})^{N_f+1}\Gamma(-N_f-1,2\hat{\alpha})\,. \tag{C.15}$$

For $\nu \neq 0$ we first analyze the two integrals in eq. (4.34) for $\hat{m} \to 0$. For small argument $\hat{m}$ and $\nu > 0$ the I-Bessel function goes to zero as given by eq. (C.1), and hence the first integral in eq. (4.34) vanishes because the integrand goes to zero like $\hat{m}^\nu$. The second integral in eq. (4.34) trivially vanishes because the integration range is empty. Therefore, the limit of the average phase factor for $\hat{m} \to 0$ is completely determined by the new Δ-term (4.33). It is interesting to note that the contributions to the phase of the determinant in the chiral limit originate from different terms for $\nu = 0$ and $\nu \neq 0$. Equation (C.8) becomes

$$\left\langle e_s^{2i\theta} \right\rangle_{\nu>0,\hat{m}=0} = \frac{e^{-2\hat{\alpha}}}{(\nu+N_f)!} \lim_{\hat{m}\to 0} \sum_{i,j=0}^{i+j\leq\nu-1} \frac{(\nu-1-i)!(\nu+N_f-j)!}{(\nu-1-i-j)!i!j!} \left(\frac{\hat{m}^2}{8\hat{\alpha}}\right)^i (2\hat{\alpha})^j\,. \tag{C.16}$$

In this double sum only the terms with $i = 0$ will contribute when $\hat{m} \to 0$ so that

$$\left\langle e_s^{2i\theta} \right\rangle_{\nu>0,\hat{m}=0} = e^{-2\hat{\alpha}} \sum_{j=0}^{\nu-1} \frac{(\nu-j)_{N_f+1}}{(\nu)_{N_f+1}} \frac{(2\hat{\alpha})^j}{j!}\,, \tag{C.17}$$

where we introduced the Pochhammer symbol

$$(a)_n \equiv a(a+1)\cdots(a+n-1) \quad \text{with} \quad (a)_0 = 1 \tag{C.18}$$

to simplify the notation. For $\nu = 1$ we notice the intriguing fact that the chiral limit of the phase factor is independent of the number of flavors, i.e., $\left\langle e_s^{2i\theta} \right\rangle_{\nu=1,\hat{m}=0} = e^{-2\hat{\alpha}}$.

Eq. (C.17) can be expressed in terms of incomplete gamma functions. To do so we note that using the Vandermonde convolution [38]

$$(a+b)_n = \sum_{k=0}^{n} \binom{n}{k} (a)_{n-k}(b)_k \tag{C.19}$$

and the identity

$$(-a)_n = (-1)^n (a-n+1)_n\,, \tag{C.20}$$

we can rewrite the coefficients of eq. (C.17) as

$$\frac{(\nu-j)_{N_f+1}}{(\nu)_{N_f}} = \sum_{k=0}^{N_f+1} (-)^k \binom{N_f+1}{k} \frac{(j-k+1)_k}{(\nu+N_f+1-k)_k}\,. \tag{C.21}$$

After substituting this expression in eq. (C.17) we find

$$\left\langle e_s^{2i\theta} \right\rangle_{\nu>0,\hat{m}=0} = e^{-2\hat{\alpha}} \sum_{k=0}^{\min(N_f+1,\nu-1)} (-)^k \binom{N_f+1}{k} \frac{1}{(\nu+N_f+1-k)_k} \sum_{j=k}^{\nu-1} (j-k+1)_k \frac{(2\hat{\alpha})^j}{j!}. \tag{C.22}$$

JHEP03(2009)100

Because $(j-k+1)_k = 0$ for $k > j$ only terms with $k \leq j$ contribute to the sum in eq. (C.21). Therefore the second sum in eq. (C.22) starts with $j = k$. Moreover, because $j \leq \nu - 1$ only terms with $k \leq \nu - 1$ contribute, which explains the upper limit of the first sum. Using the series expansion of the incomplete gamma function with positive integer first argument [37, eq. (8.352.2)],

$$\Gamma(n,z) = (n-1)!e^{-z}\sum_{j=0}^{n-1}\frac{z^j}{j!}\,, \tag{C.23}$$

eq. (C.22) can be simplified to

$$\left\langle e_s^{2i\theta}\right\rangle_{\nu>0,\hat{m}=0} = \frac{1}{(\nu+N_f)!}\sum_{k=0}^{\min(N_f+1,\nu-1)}(-)^k\binom{N_f+1}{k}(\nu-k)_{N_f+1}(2\hat{\alpha})^k\Gamma(\nu-k,2\hat{\alpha})\,. \tag{C.24}$$

Because $(\nu-k)_{N_f+1} = 0$ for $k \geq \nu$ the sum in eq. (C.24) can be extended to N_f+1 for any $\nu \geq 1$. In this case, for $n \leq 0$ eq. (C.23) should be replaced by the usual integral definition (C.13) of $\Gamma(n,z)$. Thus

$$\left\langle e_s^{2i\theta}\right\rangle_{\nu>0,\hat{m}=0} = \frac{1}{(\nu+N_f)!}\sum_{k=0}^{N_f+1}(-)^k\binom{N_f+1}{k}(\nu-k)_{N_f+1}(2\hat{\alpha})^k\Gamma(\nu-k,2\hat{\alpha}) \tag{C.25}$$

for any N_f and $\nu \geq 1$. Even though eq. (C.25) was derived for $\nu > 0$, it can formally be continued to $\nu = 0$. In this case we have $(-k)_{N_f+1} = 0$ for $k = 0,\ldots,N_f$ so that only the term with $k = N_f+1$ contributes to the sum. We obtain

$$\lim_{\nu\to 0}\left\langle e_s^{2i\theta}\right\rangle_{\nu>0,\hat{m}=0} = (N_f+1)(2\hat{\alpha})^{N_f+1}\Gamma(-N_f-1,2\hat{\alpha})\,. \tag{C.26}$$

This reproduces, somewhat surprisingly, the correct $\nu = 0$ result (C.15), even though it originates from a different term in eq. (4.34).

D Thermodynamic limit

The thermodynamic limit is defined by $\hat{\alpha} = \mu^2F^2V \to \infty$, $\hat{m} = mV\Sigma \to \infty$, and $\hat{m}_f = m_fV\Sigma \to \infty$ for $f = 1,\ldots,N_f$. As in section 5.2, we assume for simplicity that $\hat{m} = \hat{m}_1 = \ldots = \hat{m}_{N_f}$. In the following we show that for $2\hat{\alpha}/\hat{m} < 1$, the phase factor in the thermodynamic limit is given by

$$\left\langle e_s^{2i\theta}\right\rangle^{\text{th}} = \left(1-\frac{2\hat{\alpha}}{\hat{m}}\right)^{N_f+1}\,. \tag{D.1}$$

The starting point is eq. (3.30) for the phase factor in the unquenched case with N_f dynamical quarks of equal masses. We now compute the thermodynamic limit of the Wronskian $W_n(k_1,\ldots,k_n)$. Starting from the definition $I_{\nu,k}(\hat{m}) = \hat{m}^kI_{\nu+k}(\hat{m})$ it is easy to show that the p-th derivative is given by

$$I_{\nu,k}^{(p)}(\hat{m}) = \sum_{q=0}^{p}\binom{p}{q}\frac{k!}{(k-p+q)!}m^{k-p+q}I_{\nu+k}^{(q)}(\hat{m})\,, \tag{D.2}$$

where the latter expression only contains derivatives of the I-Bessel function. After substituting this expansion in the Wronskian determinant and using the asymptotic expansion

$$I_\nu(\hat{m}) = \frac{e^{\hat{m}}}{\sqrt{2\pi\hat{m}}}\left(1+\sum_{j=1}^{\infty}\frac{a_j(\nu)}{\hat{m}^j}\right)+e^{-\hat{m}}(\cdots) \tag{D.3}$$

of the I-Bessel function one can show, using basic properties of determinants, that in the thermodynamic limit only the $q=0$ term of eq. (D.2) contributes to leading order so that

$$W_n(k_1,\ldots,k_n) \sim \left(\frac{e^{\hat{m}}}{\sqrt{2\pi}}\right)^n \hat{m}^{\sum_i k_i - n^2/2}\Delta_n(k_1,\ldots,k_n) \tag{D.4}$$

for arbitrary $\{k_i\}$, where $\Delta_n(k_1,\ldots,k_n)$ is a Vandermonde determinant. Using this expression and eq. (C.6), the Wronskian in the denominator of eq. (3.30) becomes

$$W_{N_f}(0,1,\ldots,N_f-1) \sim \left(\frac{e^{\hat{m}}}{\sqrt{2\pi\hat{m}}}\right)^{N_f}\prod_{\ell=1}^{N_f-1}\ell!\,. \tag{D.5}$$

In the thermodynamic limit $\mathcal{H}^{\text{th}}_{\nu,k}(\hat{\alpha},\hat{m})$ can be computed using eq. (C.2) of ref. [28], resulting in

$$\mathcal{H}^{\text{th}}_{\nu,k}(\hat{\alpha},\hat{m}) \sim \sqrt{\frac{\pi}{2\hat{m}}}(-)^k\hat{m}^k\left(1-\frac{4\hat{\alpha}}{\hat{m}}\right)^k e^{-\hat{m}}\,, \tag{D.6}$$

which is independent of ν. To compute the thermodynamic limit of the Wronskians in eq. (3.31) we use

$$\begin{aligned}&\Delta_{N_f+1}(0,\ldots,k-1,k+1,\ldots,N_f+1) = \frac{\prod_{\ell=1}^{N_f+1}\ell!}{(N_f+1-k)!k!}\\ &\text{and}\sum_{\substack{i=0\\ i\neq k}}^{N_f+1} i = \frac{1}{2}(N_f+2)(N_f+1)-k\end{aligned} \tag{D.7}$$

to show that

$$W_{N_f+1}(0,\ldots,k-1,k+1,\ldots,N_f+1) \sim \left(\frac{e^{\hat{m}}}{\sqrt{2\pi}}\right)^{N_f+1}\hat{m}^{\frac{N_f+1}{2}-k}\frac{\prod_{\ell=1}^{N_f+1}\ell!}{(N_f+1-k)!k!}\,. \tag{D.8}$$

After substituting eqs. (D.6) and (D.8), the thermodynamic limit of eq. (3.31) becomes

$$\mathcal{W}_{N_f}(\hat{\alpha},\hat{m}) \sim \frac{1}{2}\left(\frac{e^{\hat{m}}}{\sqrt{2\pi}}\right)^{N_f}\hat{m}^{\frac{N_f}{2}}\left(\prod_{\ell=1}^{N_f+1}\ell!\right)\sum_{k=0}^{N_f+1}\frac{1}{(N_f+1-k)!k!}\left(1-\frac{4\hat{\alpha}}{\hat{m}}\right)^k\,. \tag{D.9}$$

From the binomial theorem we know that

$$\sum_{k=0}^{n}\frac{x^k}{(n-k)!k!} = \frac{(1+x)^n}{n!}\,, \tag{D.10}$$

and hence

$$\mathcal{W}_{N_f}(\hat{\alpha},\hat{m}) \sim 2^{N_f}\left(\frac{e^{\hat{m}}}{\sqrt{2\pi}}\right)^{N_f}\hat{m}^{\frac{N_f}{2}}\left(\prod_{\ell=1}^{N_f}\ell!\right)\left(1-\frac{2\hat{\alpha}}{\hat{m}}\right)^{N_f+1}. \tag{D.11}$$

After substituting eqs. (D.11) and (D.5) in eq. (3.30) we find the thermodynamic limit for the phase factor,

$$\left\langle e_s^{2i\theta}\right\rangle^{\text{th}} = \frac{1}{(2\hat{m})^{N_f}N_f!}\frac{2^{N_f}\left(\frac{e^{\hat{m}}}{\sqrt{2\pi}}\right)^{N_f}\hat{m}^{\frac{N_f}{2}}\left(\prod_{\ell=1}^{N_f}\ell!\right)\left(1-\frac{2\hat{\alpha}}{\hat{m}}\right)^{N_f+1}}{\left(\prod_{\ell=1}^{N_f-1}\ell!\right)\left(\frac{e^{\hat{m}}}{\sqrt{2\pi\hat{m}}}\right)^{N_f}}, \tag{D.12}$$

which simplifies to $(1-2\hat{\alpha}/\hat{m})^{N_f+1}$ as given in eq. (D.1).

E Numerical random matrix simulations

In this appendix we describe the numerical simulations of random matrices used to verify the analytical results derived in the main body of the paper, for both trivial and nontrivial topology. This procedure also illustrates the potential usefulness of numerical simulations in cases where analytical results would not be immediately accessible.

We performed numerical simulations of random matrices in the chiral GUE with chemical potential for the quenched case. As mentioned in eq. (2.1), these random matrices can be constructed as

$$D(\mu) = \begin{pmatrix} 0 & i\Phi+\mu\Psi \\ i\Phi^\dagger+\mu\Psi^\dagger & 0 \end{pmatrix}, \tag{E.1}$$

where Φ and Ψ are complex $(N+\nu)\times N$ matrices generated according to the Gaussian weight function

$$\begin{aligned} w(X) \propto \exp(-N\,\mathrm{tr}\,X^\dagger X) &= \exp\Big(-N\sum_{k\ell}|X_{k\ell}|^2\Big) \\ &= \prod_{k\ell}\exp\Big(-N(\mathrm{Re}\,X_{k\ell})^2\Big)\exp\Big(-N(\mathrm{Im}\,X_{k\ell})^2\Big). \end{aligned} \tag{E.2}$$

The last expression shows that the real and imaginary parts of each matrix element are i.i.d. random numbers drawn from the Gaussian distribution

$$w(x) \propto \exp\left(-Nx^2\right) \tag{E.3}$$

with standard deviation $1/\sqrt{2N}$.

As we want to investigate the microscopic limit of the theory, we will keep $\hat{\alpha}=2N\alpha$ and $\hat{m}=2Nm$ constant, while taking N large enough to approach the microscopic limit, in which $N\to\infty$. Hence, when generating and diagonalizing the matrices from eq. (E.1), the chemical potential will be scaled as $\mu=\sqrt{\hat{\alpha}/2N}$. Each random matrix $D(\mu)$ is then diagonalized and the real part of the phase factor of its determinant computed with

$$\cos 2\theta = \cos\left[2\sum_{i=1}^{2N+\nu}\arg(\lambda_i+m)\right], \tag{E.4}$$

where the λ_i are the eigenvalues and $m = \hat{m}/2N$. For a sample with $N_{\rm s}$ random matrices the real part of the average phase factor will be given by

$$\overline{\cos 2\theta}(\nu, \hat{\alpha}, \hat{m}) = \frac{1}{N_{\rm s}} \sum_{j=1}^{N_{\rm s}} \cos 2\theta_j \,, \tag{E.5}$$

where θ_j is the phase of the determinant of the j-th random matrix in the sample, given by eq. (E.4). For simplicity we have omitted the subscript s (for the microscopic limit) on $\cos 2\theta$. The average of the imaginary part will be zero within the statistical error because of the symmetry properties of the ensemble and is therefore disregarded in our analysis.

The chiral symmetry of the matrix can be used to improve the efficiency of the computer implementation by transforming the $(2N + \nu) \times (2N + \nu)$ diagonalization problem to one of size $N \times N$. Let us first rewrite eq. (E.1) as

$$D(\mu) = \begin{pmatrix} 0 & A \\ B & 0 \end{pmatrix} . \tag{E.6}$$

The eigenvalue equation

$$D(\mu)v = \lambda v \tag{E.7}$$

can then be written as

$$\begin{pmatrix} 0 & A \\ B & 0 \end{pmatrix} \begin{pmatrix} v_1 \\ v_2 \end{pmatrix} = \lambda \begin{pmatrix} v_1 \\ v_2 \end{pmatrix} , \quad \text{or} \quad \begin{cases} Av_2 = \lambda v_1 \,, \\ Bv_1 = \lambda v_2 \end{cases} \tag{E.8}$$

with complex eigenvalues λ and eigenvector decomposition $v = (v_1, v_2)$, where v_1 and v_2 are complex vectors with $(N + \nu)$ and N elements, respectively. Without fine-tuning $D(\mu)$ has exactly ν zero modes that obey the two homogeneous linear systems

$$\begin{cases} Av_2 = 0 \,, \\ Bv_1 = 0 \,. \end{cases} \tag{E.9}$$

The first system contains $N + \nu$ linear equations with N variables, and the second one N equations with $N + \nu$ variables. If both A and B are of rank N (no fine-tuning), the first homogeneous system only has solutions $v_2 = 0$, while the second system is underconstrained and has ν linearly independent solutions for v_1. Hence the zero modes will be represented by ν eigenvectors $(v_{1k}, 0)$ with $k = 1, \ldots, \nu$.

Moreover, it is clear from eq. (E.8) that each nonzero eigenvalue λ with eigenvector (v_1, v_2) will be paired with an eigenvalue $-\lambda$ with eigenvector $(v_1, -v_2)$. This is a consequence of the chiral symmetry of the problem.

These properties of the spectrum of $D(\mu)$ will now be used to transform the diagonalization problem from order $2N + \nu$ to order N. For this, let us first multiply eq. (E.8) from the left with $D(\mu)$,

$$D^2(\mu)v = \begin{pmatrix} AB & 0 \\ 0 & BA \end{pmatrix} \begin{pmatrix} v_1 \\ v_2 \end{pmatrix} = \lambda^2 \begin{pmatrix} v_1 \\ v_2 \end{pmatrix} , \tag{E.10}$$

JHEP03(2009)100

where AB is an $(N+\nu)\times(N+\nu)$ matrix and BA has dimension $N\times N$. Clearly, each nonzero eigenvalue λ^2 of AB (with eigenvector v_1) is also an eigenvalue of BA (with eigenvector v_2). However, AB has ν additional eigenvalues, which necessarily correspond to the zero modes $(v_{1k},0)$ satisfying eq. (E.9).

This can be used to expedite the numerical simulations. It suffices to diagonalize the $N\times N$ matrix BA to find the N nonzero eigenvalues λ_i^2. We then know that the eigenvalues of $D(\mu)$ are the N pairs $(\lambda_i,-\lambda_i)$ supplemented by ν eigenvalues equal to zero. The determinant for a fermion of mass m will then be given by

$$\det(D(\mu)+m)=m^\nu\prod_{i=1}^{N}(m^2-\lambda_i^2)\,, \tag{E.11}$$

and the real part of its phase factor is

$$\cos 2\theta=\cos\left[2\sum_{i=1}^{N}\arg(m^2-\lambda_i^2)\right], \tag{E.12}$$

which replaces eq. (E.4) in our practical simulations. Note that the cost of the additional multiplication of an $N\times(N+\nu)$ by an $(N+\nu)\times N$ matrix to construct the product BA is negligible compared to the cost of the diagonalization.

References

[1] M.A. Stephanov, *QCD phase diagram: an overview*, *PoS* **LAT2006** (2006) 024 [hep-lat/0701002] [SPIRES].

[2] J. Ambjørn, K.N. Anagnostopoulos, J. Nishimura and J.J.M. Verbaarschot, *The factorization method for systems with a complex action -a test in Random Matrix Theory for finite density QCD-*, *JHEP* **10** (2002) 062 [hep-lat/0208025] [SPIRES].

[3] J. Ambjørn, K.N. Anagnostopoulos, J. Nishimura and J.J.M. Verbaarschot, *Non-commutativity of the zero chemical potential limit and the thermodynamic limit in finite density systems*, *Phys. Rev.* **D 70** (2004) 035010 [hep-lat/0402031] [SPIRES].

[4] M. Troyer and U.-J. Wiese, *Computational complexity and fundamental limitations to fermionic quantum Monte Carlo simulations*, *Phys. Rev. Lett.* **94** (2005) 170201 [cond-mat/0408370] [SPIRES].

[5] J.C. Osborn, K. Splittorff and J.J.M. Verbaarschot, *Chiral symmetry breaking and the Dirac spectrum at nonzero chemical potential*, *Phys. Rev. Lett.* **94** (2005) 202001 [hep-th/0501210] [SPIRES].

[6] M. Imachi, Y. Shinno and H. Yoneyama, *Sign problem and MEM in lattice field theory with the θ term*, *Prog. Theor. Phys.* **115** (2006) 931 [hep-lat/0602009] [SPIRES].

[7] K. Fukushima and Y. Hidaka, *A model study of the sign problem in the mean-field approximation*, *Phys. Rev.* **D 75** (2007) 036002 [hep-ph/0610323] [SPIRES].

[8] S. Ejiri, *On the existence of the critical point in finite density lattice QCD*, *Phys. Rev.* **D 77** (2008) 014508 [arXiv:0706.3549] [SPIRES].

[9] G. Aarts, *Can stochastic quantization evade the sign problem? — The relativistic Bose gas at finite chemical potential*, arXiv:0810.2089 [SPIRES].

JHEP03(2009)100

[10] E.V. Shuryak and J.J.M. Verbaarschot, *Random matrix theory and spectral sum rules for the Dirac operator in QCD*, *Nucl. Phys.* **A 560** (1993) 306 [hep-th/9212088] [SPIRES].

[11] J.J.M. Verbaarschot and T. Wettig, *Random matrix theory and chiral symmetry in QCD*, *Ann. Rev. Nucl. Part. Sci.* **50** (2000) 343 [hep-ph/0003017] [SPIRES].

[12] J.J.M. Verbaarschot, *QCD, chiral random matrix theory and integrability*, hep-th/0502029 [SPIRES].

[13] F. Basile and G. Akemann, *Equivalence of QCD in the ε-regime and chiral Random Matrix Theory with or without chemical potential*, *JHEP* **12** (2007) 043 [arXiv:0710.0376] [SPIRES].

[14] M.A. Stephanov, *Random matrix model of QCD at finite density and the nature of the quenched limit*, *Phys. Rev. Lett.* **76** (1996) 4472 [hep-lat/9604003] [SPIRES].

[15] G. Akemann, *Microscopic correlation functions for the QCD Dirac operator with chemical potential*, *Phys. Rev. Lett.* **89** (2002) 072002 [hep-th/0204068] [SPIRES].

[16] G. Akemann, *The solution of a chiral random matrix model with complex eigenvalues*, *J. Phys.* **A 36** (2003) 3363 [hep-th/0204246] [SPIRES].

[17] J.C. Osborn, *Universal results from an alternate random matrix model for QCD with a baryon chemical potential*, *Phys. Rev. Lett.* **93** (2004) 222001 [hep-th/0403131] [SPIRES].

[18] G. Akemann, *Matrix models and QCD with chemical potential*, *Int. J. Mod. Phys.* **A 22** (2007) 1077 [hep-th/0701175] [SPIRES].

[19] G. Akemann and T. Wettig, *QCD Dirac operator at nonzero chemical potential: lattice data and matrix model*, *Phys. Rev. Lett.* **92** (2004) 102002 [hep-lat/0308003] [SPIRES].

[20] J.C.R. Bloch and T. Wettig, *Overlap Dirac operator at nonzero chemical potential and random matrix theory*, *Phys. Rev. Lett.* **97** (2006) 012003 [hep-lat/0604020] [SPIRES].

[21] G. Akemann, J.C.R. Bloch, L. Shifrin and T. Wettig, *Individual complex Dirac eigenvalue distributions from random matrix theory and lattice QCD at nonzero chemical potential*, *Phys. Rev. Lett.* **100** (2008) 032002 [arXiv:0710.2865] [SPIRES].

[22] P.H. Ginsparg and K.G. Wilson, *A remnant of chiral symmetry on the lattice*, *Phys. Rev.* **D 25**(1982) 2649.

[23] R. Narayanan and H. Neuberger, *Chiral determinant as an overlap of two vacua*, *Nucl. Phys.* **B 412** (1994) 574 [hep-lat/9307006] [SPIRES].

[24] R. Narayanan and H. Neuberger, *A construction of lattice chiral gauge theories*, *Nucl. Phys.* **B 443** (1995) 305 [hep-th/9411108] [SPIRES].

[25] H. Neuberger, *Exactly massless quarks on the lattice*, *Phys. Lett.* **B 417** (1998) 141 [hep-lat/9707022] [SPIRES].

[26] M. Lüscher, *Exact chiral symmetry on the lattice and the Ginsparg-Wilson relation*, *Phys. Lett.* **B 428** (1998) 342 [hep-lat/9802011] [SPIRES].

[27] J.C.R. Bloch and T. Wettig, *Domain-wall and overlap fermions at nonzero quark chemical potential*, *Phys. Rev.* **D 76** (2007) 114511 [arXiv:0709.4630] [SPIRES].

[28] K. Splittorff and J.J.M. Verbaarschot, *The QCD sign problem for small chemical potential*, *Phys. Rev.* **D 75** (2007) 116003 [hep-lat/0702011] [SPIRES].

[29] Y.V. Fyodorov and E. Strahov, *An exact formula for general spectral correlation function of random Hermitian matrices*, *J. Phys.* **A 36** (2003) 3203 [math-ph/0204051] [SPIRES].

JHEP03(2009)100

[30] E. Strahov and Y.V. Fyodorov, *Universal results for correlations of characteristic polynomials: Riemann-Hilbert approach*, *Commun. Math. Phys.* **241** (2003) 343 [math-ph/0210010] [SPIRES].

[31] G. Akemann and A. Pottier, *Ratios of characteristic polynomials in complex matrix models*, *J. Phys.* **A 37** (2004) L453 [math-ph/0404068] [SPIRES].

[32] G. Akemann, J.C. Osborn, K. Splittorff and J.J.M. Verbaarschot, *Unquenched QCD Dirac operator spectra at nonzero baryon chemical potential*, *Nucl. Phys.* **B 712** (2005) 287 [hep-th/0411030] [SPIRES].

[33] M.C. Bergere, *Biorthogonal polynomials for potentials of two variables and external sources at the denominator*, hep-th/0404126 [SPIRES].

[34] M. Abramowitz and I.A. Stegun, *Handbook of mathematical functions with formulas, graphs, and mathematical tables*, tenth edition, GPO printing ed. (1964).

[35] A. Erdélyi ed., *Higher transcendental functions. Volume II: Bateman manuscript project*, McGraw-Hill Book Company Inc. (1953).

[36] J.C. Osborn, K. Splittorff and J.J.M. Verbaarschot, *Chiral condensate at nonzero chemical potential in the microscopic limit of QCD*, *Phys. Rev.* **D 78** (2008) 065029 [arXiv:0805.1303] [SPIRES].

[37] I. Gradshteyn and I. Ryzhik, *Table of integrals, series and products*, 5th ed., Academic Press, San Diego U.S.A. (1994); http://www.mathtable.com/errata/gr6_errata.pdf.

[38] L. Comtet, *Advanced combinatorics: the art of finite and infinite expansions*, D. Reidel Publishing Company (1974).

JHEP03(2009)100